

We are IntechOpen, the world's leading publisher of Open Access books Built by scientists, for scientists

4,800

Open access books available

122,000

International authors and editors

135M

Downloads

Our authors are among the

154

Countries delivered to

TOP 1%

most cited scientists

12.2%

Contributors from top 500 universities



WEB OF SCIENCE™

Selection of our books indexed in the Book Citation Index
in Web of Science™ Core Collection (BKCI)

Interested in publishing with us?
Contact book.department@intechopen.com

Numbers displayed above are based on latest data collected.
For more information visit www.intechopen.com



Microwave Hydrothermal and Solvothermal Processing of Materials and Compounds

Boris I. Kharisov, Oxana V. Kharissova and Ubaldo Ortiz Méndez

Additional information is available at the end of the chapter

<http://dx.doi.org/10.5772/45626>

1. Introduction

Hydrothermal synthesis (or hydrothermal method) includes the various techniques of fabrication or crystallizing substances from high-temperature aqueous solutions at high vapor pressures. In case of crystallization processes, the hydrothermal synthesis can be defined as a method of synthesis of single crystals that depends on the solubility of minerals in hot water under high pressure. The crystal growth is performed in an apparatus consisting of a steel pressure vessel called autoclave, in which a nutrient is supplied along with water. A gradient of temperature is maintained at the opposite ends of the growth chamber so that the hotter end dissolves the nutrient and the cooler end causes seeds to take additional growth.

Nowadays, combinations of different techniques are very common and the hydrothermal method is not an exception. Hydrothermal hybrid techniques are frequently applied for synthesis of materials (including nanomaterials) and chemical compounds, mainly inorganics. In order to additionally enhance the reaction kinetics or the ability to make new materials, a great amount of work has been done to hybridize the hydrothermal technique with microwaves (MW) (*microwave-hydrothermal processing*), electrochemistry (*hydrothermal-electrochemical synthesis*), ultrasound (*hydrothermal-sonochemical synthesis*), mechanochemistry (*mechanochemicalhydrothermal synthesis*), optical radiation (*hydrothermal-photochemical synthesis*), and hot-pressing (*hydrothermal hot pressing*) (Suchanek & Riman, 2006). Hydrothermal method itself, microwave-hydrothermal and microwave-solvothermal methods are, in particular, truly low-temperature methods for the preparation of nanophase materials of different sizes and shapes. These methods save energy and are environmentally friendly, because the reactions take place in closed isolated system conditions. The nanophase materials can be produced in either a batch or continuous process using the above methods. In contrast to the conventional heating hydro/solvothermal method, which

requires a long time (typically half to several days) and high electric power (over a thousand Watts), microwave-assisted heating is a greener approach to synthesize materials in a shorter time (several minutes to hours) and with lower power consumption (hundreds of Watts) as a consequence of directly and uniformly heating the contents. Particular aspects of these techniques were examined in several reviews (Shangzhao Shi & Jiann-Yang Hwang, 2003; Komarneni, 2003; Komarneni & Katsuki, 2002) and a book chapter (Guiotoku et al., 2011).

In this Chapter, we try to describe briefly main aspects of hydro/solvothermal processes under simultaneous microwave heating (H-MW or S-MW). Reactions, carried out by consecutive application of hydro/solvothermal and microwave treatment, are out of scope of this study.

2. Typical equipment

Typical commercial equipment, used for MW hydro/solvothermal processing, is shown in Fig. 1. Its cost is usually about 30,000 USD. Several reports describe also home-made combinations of MW-heating and hydro/solvothermal reactions.



Figure 1. Typical equipment (MARS), used for MW hydro/solvothermal processing.

3. Inorganic compounds

The H-MW method was used for preparation of free or supported *elemental metals* (Cu, Ni, Co, Ag) long ago (Komarneni et al., 1995). Thus, microwave-hydrothermal processing in combination with polyol process was used to prepare Ag⁰-, Pt⁰- or Pd⁰-intercalated montmorillonite (Komarneni, Hussein, et al., 1995). Sub-nanometer metal clusters were introduced into the interlayers while some larger metal particles of 5-100 nm were crystallized on the external surfaces. The small metal clusters in the interlayers and on the external surfaces may be useful in certain catalytic applications. The reduction of chlorocomplexes of gold(III) from muriatic solutions by nanocrystal powders of palladium and platinum at 110 and 130°C under H-MW conditions was studied, revealing Au-Pd and

Au-Pt bimetallic particles with a core-shell structure according to the scheme shown in Fig. 2 (Belousov et al, 2011). The obtained particles had a core of the metal reductant covered with a substitutional solid (Au, Pd) solution in case of palladium, and isolated by a gold layer in the case of platinum. It was shown by the example of the Au-Pd system that the use of microwave irradiation allowed one not only to accelerate the synthesis of particles but also to obtain more homogeneous materials in comparison with conventional heating. In addition, magnetic FeNi₃ nanochains were synthesized by reducing iron(III) acetylacetonate and nickel(II) acetylacetonate with hydrazine in ethylene glycol solution without any template according to the mechanism shown in Fig. 3 (Jia et al., 2010). The size of the aligned nanospheres in the magnetic FeNi₃ chains could be adjusted from 150 to 550 nm by increasing the amounts of the precursors. Magnetic measurement revealed that the FeNi₃ nanochains showed enhanced coercivity and saturation magnetization. As an example of core-shell-type gold nanoparticles, the Au/SnO₂ core-shell structure was synthesized using the H-MW method (Yu & Dutta, 2011). In MW preparation, the peak position of the UV-visible plasmon absorption band of Au nanoparticles was red shifted from 520 to 543 nm, due to the formation of an SnO₂ shell. An SnO₂ shell (thickness 10-12 nm) formation was complete within 5 min.

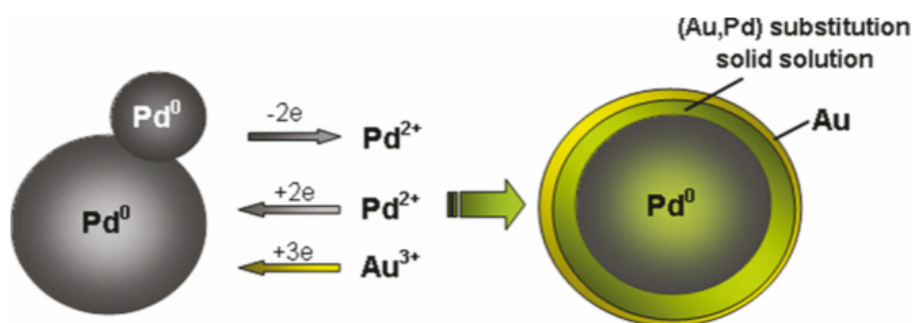


Figure 2. Core-shell Au/Pd particle formation scheme. With permission.

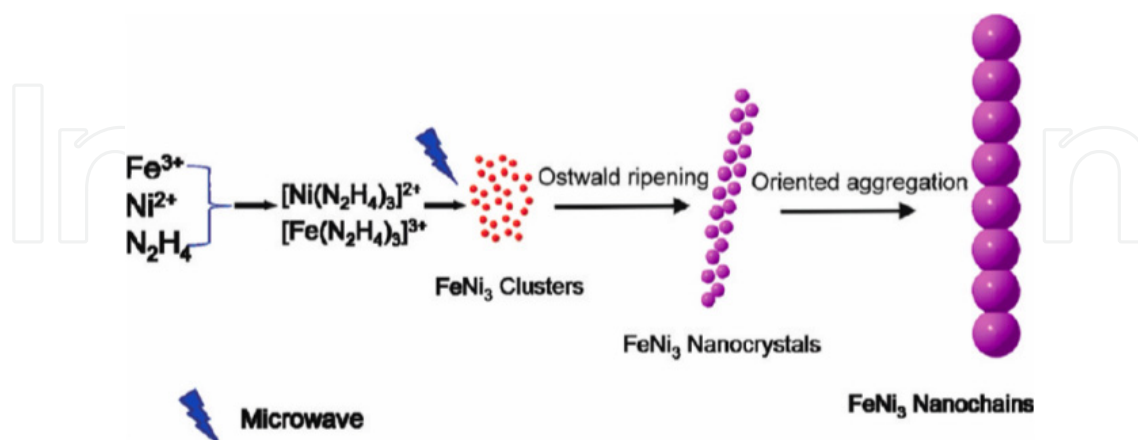


Figure 3. Illustration of a proposed mechanism for the formation of FeNi₃ nanochains. With permission.

Among *metal oxides*, TiO₂ is the compound, received obviously main attention of researchers due to its numerous applications, in particular in nanostructured forms. Similar applied methods led to a variety of its distinct crystalline phases obtained in different reports. Thus,

nanoparticles of *brookite*-type TiO_2 were prepared at 200°C (H-MW-heating time 5 min) for 0-60 min starting from the titanium peroxo glycolate complex in basic solution (Morishima et al., 2007). The activity in photodecomposition of oxalic acid by the samples prepared using H-MW technique was higher than activities of brookite nanoparticles prepared by the conventional hydrothermal method. On the contrary, mesoporous titanium dioxide with highly crystalline *anatase* phase and high surface area, a promising material for energy and environmental application, was obtained (Huang et al., 2011) *via* H-MW route using stable and water-soluble titanium citrate complexes as the precursors. It was shown that the synthesized TiO_2 contained mainly anatase phase with crystallite size of 5.0-8.6 nm at various hydrothermal temperatures and durations ranging from 150 to 180°C and from 30 to 120 min, respectively. The mesoporous nanocrystals synthesized at 180°C were then used to prepare the TiO_2 photoelectrode using screen-printing deposition method. The MW180-120-based TiO_2 photoanode exhibited a good efficiency on photocurrent conversion and the conversion efficiency was in the range 4.8-7.1%, depending on active area and film thickness. In addition, TiO_2 of the shuttle-like *rutile* phase (10 nm) was prepared using TiCl_4 and HCl by H-MW method (Chen et al., 2008). Interestingly, the use of H-MW method resulted in the formation of TiO_2 *nanotubes* comprising anatase and rutile phases (Sikhwivhilu et al., 2010). Conventional hydrothermal heating resulted in the formation of tubes with a titanate structure. The two methods yielded tubular structures with similar size dimensions, surface areas and morphologies. The two methods gave 100 % yields of tubes with different degrees of crystallinity. At last, the combination of sonication and H-MW (three methods at once) led to preparing fluorinated mesoporous TiO_2 *microspheres* (500 nm size) (Zhu et al., 2010). The authors achieved the fabrication of mesoporous TiO_2 , doping of fluorine by sonication and then hydrothermal treatment of a solution containing TiO_2 precursor sol and sodium fluoride.

Zinc oxide, the principal nanotechnological object, was also intensively studied and reported in distinct forms, in particular as nanobar-structured ZnO thin film (Li et al., 2011) (obtained from Zn salt solution (nitrate, chloride, acetate, and/or sulfate) and hexamethylenetetramine solution as raw materials). The wide interest in ZnO has resulted from the following fundamental characteristic features with potential applications in electronic, structural and bio-materials: direct band gap semiconductor (3.37 eV), large excitation binding energy (60 meV), near UV emission and transparent conductivity. ZnO nanorods were synthesized using zinc nitrate and methenamine aqueous solutions in a H-MW process (Shojaee et al., 2010). It was revealed that concentration of precursors and irradiation power displayed significant influences on the compaction and dimensions of the grown nanorods. The 1D ZnO nanostructures and microstructures with a hexagonal cross-section growing in the (0002) direction were obtained under H-MW method (MW 2.45 GHz) at 130°C for 30 min (de Moura et al., 2010). In addition, the intriguing results were reported (Huang, J. et al., 2008) for a facile H-MW route employing the reaction of $\text{Zn}(\text{NO}_3)_2 \cdot 6\text{H}_2\text{O}$ and NaOH to synthesize a single-crystal zinc oxide 1D nanostructure with a 3D morphology (Fig. 4). A substantial reduction in the reaction time as well as the reaction temperature is observed compared with the hydrothermal process. Fig. 5 shows a condensed illustration of the authors' strategies in the morphology control of ZnO nanostructures. First, ZnO nuclei

generally evolve into nanorods by preferential c-axis ([002] direction) oriented 1D growth. Second, nanorods can be converted into nanowires by a multiple nanorods growth along the [002] direction and simultaneous local attachment of the polar (0001) surfaces or nanospindles by an increase in diameter and local dissolution. Third, multiple nanorods grow from center results in nanodandelions. Fourth, when the crystal growth along the [002] direction is suppressed, nanoslices can be obtained due to quasi 1D growth. Finally, when multiple nanoslices grow further, nanothruster vanes can be formed by self-assembled growth. The MW-hydrothermal mechanism of ZnO nanostructures can be considered as follows (reactions 1-2):

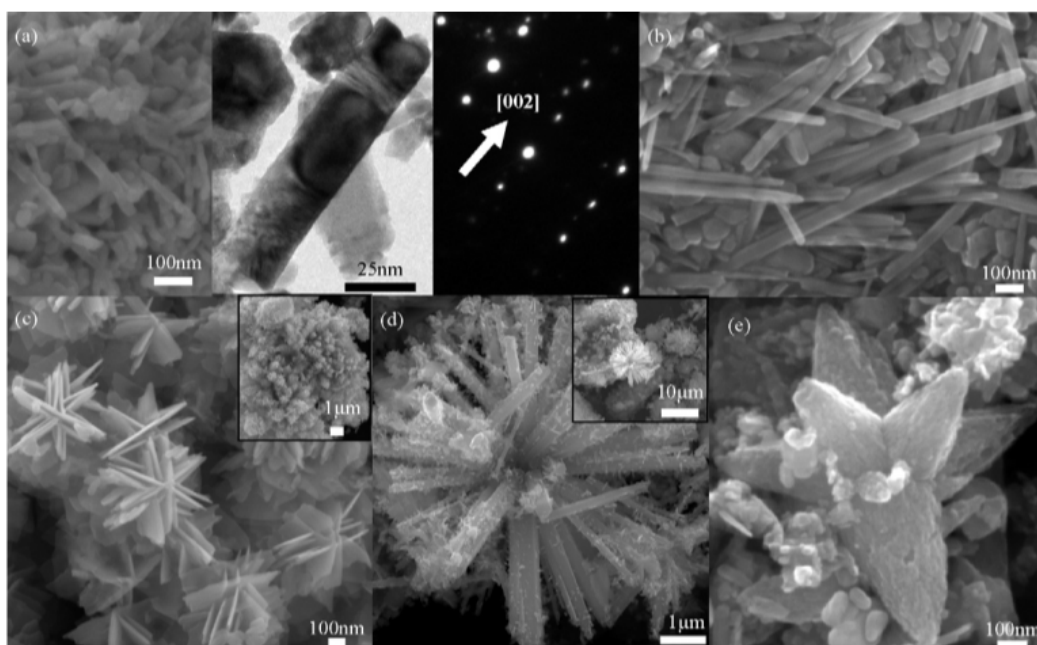
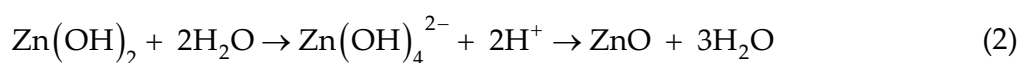
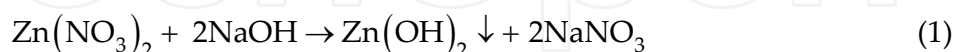


Figure 4. FE-SEM images of the ZnO nanocrystals with different morphologies: nanorods (a, temperature = 413 K, $[\text{Zn}^{2+}] = 1.6 \text{ mol L}^{-1}$, filling ratio = 70%, time = 20 min, middle: HRTEM image and right: selected area electron diffraction (SEAD) pattern), nanowires (b, temperature = 453 K, $[\text{Zn}^{2+}] = 1.6 \text{ mol L}^{-1}$, filling ratio = 70%, time = 20 min), nanothruster vanes (c, temperature = 393 K, $[\text{Zn}^{2+}] = 1.6 \text{ mol L}^{-1}$, filling ratio = 70%, time = 20 min), nanodandelions (d, temperature = 373 K, $[\text{Zn}^{2+}] = 1.6 \text{ mol L}^{-1}$, filling ratio = 70%, time = 20 min) and radial nanospindles (e, pressure = 3.0 MPa, $[\text{Zn}^{2+}] = 0.8 \text{ mol L}^{-1}$, filling ratio = 70%, time = 20 min). With permission.

Other simple and mixed/complex oxides are extensively reported. Thus, yttria stabilized zirconia (YSZ) is the main material for preparing functional device such as oxygen sensor, solid state oxide fuel cell and high temperature humidity transducer (Zhao et al., 2007). Its nanopowders were prepared by H-MW method with programmable MARS-5 microwave digester in strong basic media at temperature from 100-120°C and time from 1 h to 5 h, while the temperature is 190-250°C by conventional hydrothermal heating (CH). The result

showed that compared with CH, H-MW can reduce the reaction time, and influence the content of product. The CH and H-MW techniques were also used for production of nanocrystalline zirconium and hafnium dioxides (8-20 nm) at 180 and 250°C and highly dispersive powders of barium zirconate and hafnate at 150°C (Maksimov et al., 2008). HfO_2 was also H-MW-obtained in a rice form (Eliziari et al., 2009) according to the following reactions 3-5:

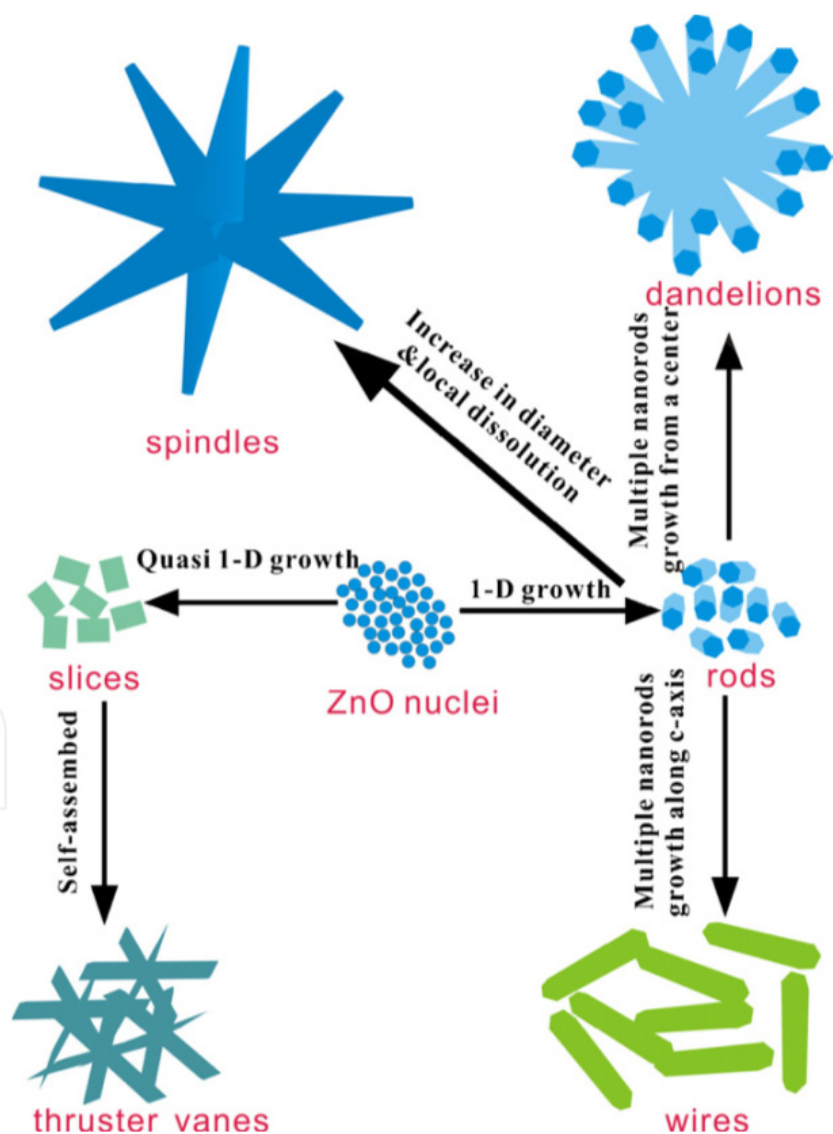
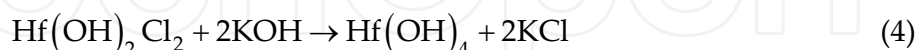
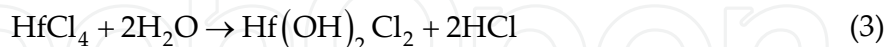


Figure 5. Schematic of the shape-controlled synthesis of ZnO nanorods, nanowires, nanothruster vanes, nanodandelions and radial nanospindles *via* a microwave hydrothermal route. With permission.

The effect of microwave radiation on the formation of smaller and uniform α -Fe₂O₃ powders from FeCl₃ solution at 100-140°C was investigated (Katsuki, 2009). As a practical application, a new red pigment on their basis for porcelain was developed. Structures of tin oxides in different oxidation states are known, for instance SnO₂ nanoparticles (Krishna & Komarneni, 2009) or SnO powders (Pires et al., 2008); the last ones were obtained by the H-MW technique using SnCl₂·2H₂O as a precursor. By changing the hydrothermal processing time, temperature, the type of mineralizing agent (NaOH, KOH, or NH₄OH) and its concentration, SnO crystals having different sizes and morphologies could be achieved. Plate-like form was found to be the characteristic morphology of growth. CuO with less-common sea urchin-like morphology is also known (Volanti et al., 2010). Single crystalline Co₃O₄ nanorods (Li, W.-h., 2008) or Co₃O₄ mesoporous nanowires (Zeng et al., 2011) with average single crystalline grain sizes of 8 nm, 12 nm, 25 nm, and 45 nm were synthesized by sintering the last nanostructure of H-MW-processed belt-Co(OH)₂ precursors at 300-500°C for 2 h. The interesting finding was made that room temperature ferromagnetism appeared at 350°C in the high orientation samples. A mixture of crystalline Co₃O₄/CoO nanorods (length of around 80 nm and an average diameter of 42 nm) with non-uniform dense distribution was synthesized by H-MW technique (Al-Tuwirqi et al., 2011). The band energy gap of the product was 1.79 eV which lies between the energy gap of CoO and that for Co₃O₄. As synthesized mixed Co₃O₄/CoO nanorods can be very useful for supercapacitor devices application. Magnetic hysteresis loops at room temperature of the as synthesized mixed oxides (Co₃O₄/CoO) nanorods exhibit typical soft magnetic behavior.

MoO₃ nanoflowers were synthesized on a Si substrate by a facility H-MW method (Wei et al., 2009). The nanoflowers consisted of tens of nanobelts and the nanobelts were about several micrometers in length, several tens to several hundreds of nanometers in width, and tens of nanometers in thickness. As-grown MoO₃ nanobelts exhibited a good field-emission property and have great potential for applications in field-emission devices. In case of tungsten oxide, its compounds with different composition were reported, for example monodisperse crystalline WO₃·2H₂O (H₂WO₄·H₂O) nanospheres, which were prepared by (+)-tartaric acid-assisted H-MW process (Sun et al., 2008), meanwhile the synthesis of crystalline W₁₈O₄₉ with nanosheet like morphology was carried out by low cost MW irradiation method without employing hydrothermal process (Hariharan et al., 2011). The W₁₈O₄₉ nanosheets had the average dimensions of the order of 250 nm in length and around 150 nm in width. The band gap energies to be 3.28 and 3.47 eV for WO₃·H₂O and W₁₈O₄₉ samples, respectively. An hierarchically structured WO₃·0.33H₂O "snowflakes" were synthesized by a template-free and H-MW method (Li, J. et al., 2011). Their particles had an oriented growth along six equivalent <100> directions in (001) plane to form the snowflakelike microstructure, which is significantly different from the sample prepared at conventional hydrothermal conditions. Moreover, microwave heating was considered by authors to accelerate the oriented crystal growth along <100> directions. Mixed Mo-W nanostructures are also known. Thus, W_{0.4}Mo_{0.6}O₃ and carbon-decorated WO_x-MoO₂ (x = 2 and 3) nanorods were synthesized (Yoon & Manthiram, 2011). The carbon-decorated WO_x-MoO₂ nanorods exhibited excellent capacity retention as the carbon provides an elastic matrix for absorbing the volume expansion-contraction smoothly and prevents aggregation

of the nanorods during cycling. In addition, solid solutions of titanium-tin oxide $\text{Ti}_x\text{Sn}_{1-x}\text{O}_2$ were prepared by H-MW method from a solution containing TiCl_3 and SnCl_4 (Yang et al., 2011). The advantage and contribution of this technique was revealed to be effective reduction of the difference in the formation rate of TiO_2 and SnO_2 , resulting in the precise control of the solid solution composition. Enlarging the crystal size of single-phase, rutile-type $\text{Ti}_x\text{Sn}_{1-x}\text{O}_2$ solid solutions can be achieved by annealing in air and the crystal phase is stable at 800°C .

A series of reports is devoted to lanthanide oxides, in particular to distinct CeO_2 nanostructures, for instance virtually nonaggregated, primarily hexagonal CeO_2 nanoparticles (Ivanov et al., 2009). In another research (Dos Santos et al., 2008), crystalline CeO_2 nanoparticles were prepared by a simple and fast H-MW method at 130°C for 20 min and then were calcinated at 500°C for 1, 2 and 4 h. Ceria powders were found to have, in this case, a spherical shape with particle size below 10 nm, a narrow distribution, and exhibit weak agglomeration. In addition, ceria hollow nanospheres composed of CeO_2 nanocrystals were synthesized *via* a template-free H-MW method (Cao et al., 2010). An Ostwald ripening mechanism (Fig. 6) coupled with a self-templated, self-assembly process, in which amorphous solid spheres are converted to crystalline nanocrystals and the latter self-assemble into hollow structures, was proposed for the formation of these ceria hollow structures, which showed an excellent adsorption capacity for heavy metal ions, for example, $22.4 \text{ mg}\cdot\text{g}^{-1}$ for As(V) and $15.4 \text{ mg}\cdot\text{g}^{-1}$ for Cr(VI). The authors noted that these ceria hollow nanospheres are also excellent supports for gold nanoparticles, forming a Au/ CeO_2 composite catalyst. Nanocrystalline Nd_2O_3 precursor particles were prepared by a H-MW route from a solution containing $\text{Nd}(\text{CH}_3\text{COO})_3\cdot\text{H}_2\text{O}$ (Zawadzki, 2008). Further thermal treatment of the as-prepared precursors resulted in the formation of the well-crystallized Nd_2O_3 (cubic or trigonal) nanoparticles with fibrous or rod-like morphology (specific surface area $130 \text{ m}^2/\text{g}$).

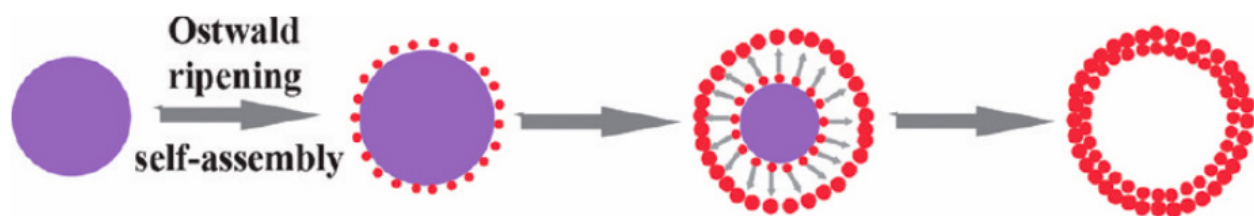


Figure 6. Illustration of the Ostwald ripening coupled self-templated, self-assembly process of the ceria precursor. With permission.

A small number of *hydroxides*, obtained by H-MW technique, are known. Thus, the CH and H-MW methods were used to synthesize layered double hydroxides (LDHs) (Wang et al., 2011). The microwave treatment LDHs (of MgAl and NiMgAl) were found to have higher crystallinity and smaller crystal sizes than the conventional hydrothermal treatment LDHs. It was indicated that the interactions of both OH^- - CO_3^{2-} and CO_3^{2-} - CO_3^{2-} in NiMgAl -LDH, obtained by H-MW technique, are weaker. Also, the thermal decomposition of OH^- and CO_3^{2-} in the NiMgAl -LDH sample, obtained by H-MW technique, occurred earlier and faster than that of other LDHs. Nanostructural β -Ni hydroxide β - $\text{Ni}(\text{OH})_2$ plates were prepared

using the H-MW method at a low temperature and short reaction times (de Moura et al., 2011). An NH_3 solution was employed as the coordinating agent, which reacts with $[\text{Ni}(\text{H}_2\text{O})_6]^{2+}$ to control the growth of $\beta\text{-Ni}(\text{OH})_2$ nuclei. It was revealed that the samples consisted of hexagonal-shaped nanoplates with a different particle size distribution. Hierarchically nanostructured $\gamma\text{-AlOOH}$ microspheres self-assembled by nanosheets were prepared *via* H-MW technique at 160°C for 30 min, by using $\text{AlCl}_3 \cdot 6\text{H}_2\text{O}$ and NaOH as raw materials and cetyltrimethyl ammonium bromide (CTAB) as surfactant, respectively (Liu et al., 2011). The morphology-contained $\gamma\text{-Al}_2\text{O}_3$ can be obtained through the thermal decomposition of $\gamma\text{-AlOOH}$ precursors at 500°C for 2 h. Both of $\gamma\text{-AlOOH}$ and $\gamma\text{-Al}_2\text{O}_3$ microspheres were used to adsorb Congo red from water solution. Cubic-shaped $\text{In}(\text{OH})_3$ particles with average size of $0.348\ \mu\text{m}$ were precipitated from a mixed aqueous solution of InCl_3 and urea by a H-MW method (Koga & Kimizu, 2008). No intermediate compound was found during the course of thermal decomposition from cubic- $\text{In}(\text{OH})_3$ to cubic- In_2O_3 . In addition, GaOOH nanorods were synthesized from $\text{Ga}(\text{NO}_3)_3$ *via* a facile H-MW method (Sun, M. et al., 2010). It was revealed that the as-synthesized sample was consisted of rod-like particles. The results for degradation of aromatic compounds (such as benzene and toluene) in an O_2 gas stream under UV light illumination demonstrated that GaOOH nanorods exhibited superior photocatalytic activity and stability as compared to commercial TiO_2 in both benzene and toluene degradation.

A considerable number of publications are devoted to H-MW fabrication of *oxygen-containing salts*, in particular to metal *titanates*, both simple as BaTiO_3 (Sun, W. et al., 2007; Nyutu et al., 2008) and more complex non-stoichiometric as $\text{Ba}_{0.75}\text{Sr}_{0.25}\text{Zr}_{0.1}\text{Ti}_{0.9}\text{O}_3$ (Chen & Luo, 2008) or $\text{Bi}_{0.5}\text{Na}_{0.5}\text{TiO}_3$ (Lv et al., 2009). Influence of reaction conditions on their synthesis and structures has been studied. Thus, the role of *in situ* stirring under H-MW conditions on the preparation of barium titanate was investigated (Komarneni & Katsuki et al., 2010). It was established that stirring under H-MW conditions in the temperature range of $150\text{--}200^\circ\text{C}$ led to enhanced crystallization of Ba titanate as revealed by yields compared to the static condition. In addition, stirring led to smaller and more uniform crystals under H-MW conditions compared to those crystallized without stirring. Nanoparticles (20–40 nm) of barium titanate doped with different amounts of Sn^{2+} consisting of single phase perovskite structure were synthesized by using a S-MW reaction (Xie et al., 2009). Ceramic bodies (Fig. 7) were obtained using a spark plasma sintering method under argon atmosphere avoiding the disproportionation and oxidation of Sn^{2+} in the air. It was considered that Sn^{2+} entered into A site of the perovskite formula, ABO_3 , because the lattice parameters decreased with increasing the amount of doped Sn^{2+} . The particle sizes were about 20–40 nm and increased with increasing the amount of doped Sn^{2+} . The H-MW method was used also to synthesize crystalline barium strontium titanate ($\text{Ba}_{0.8}\text{Sr}_{0.2}\text{TiO}_3$) nanoparticles (BST, 40–80 nm) in the temperature range of $100\text{--}130^\circ\text{C}$ (Simoes et al., 2010). Comparing this and conventional techniques, it was shown that the H-MW synthesis route is rapid, cost effective, and could serve as an alternative to obtain BST nanoparticles. In addition, as a combination of three techniques, MW-heating was applied in the sonocatalyzed hydrothermal preparation of tetragonal phase-pure lead titanate nanopowders with stoichiometric chemical composition (Tapala et al., 2008).

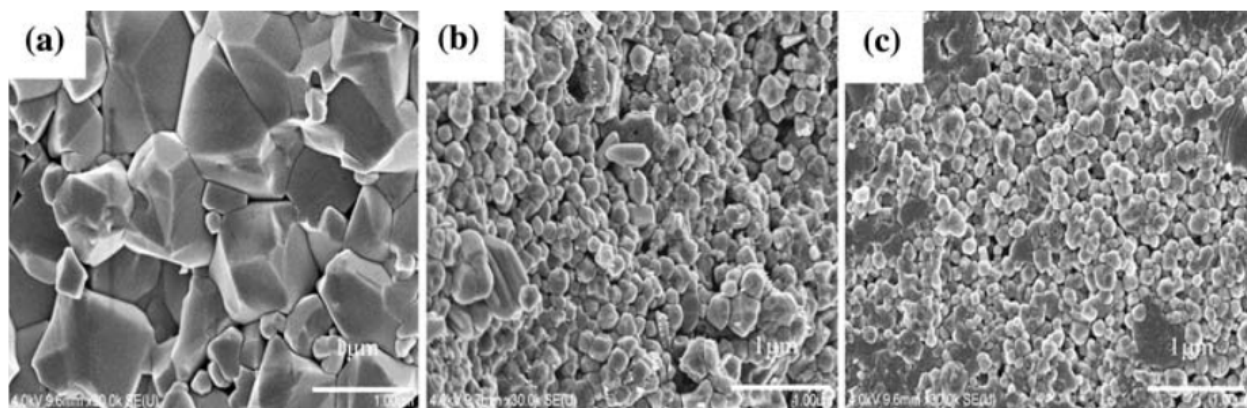


Figure 7. SEM images of a) BaTiO_3 , b) $\text{Ba}_{0.90}\text{Sn}_{0.10}\text{TiO}_3$, and c) $\text{Ba}_{0.80}\text{Sn}_{0.20}\text{TiO}_3$ ceramic body. With permission.

Related *niobates*, *molybdates* (for example SrMoO_4 (Sczancoski et al., 2008)), *zirconates*, and *tungstates* were also widely reported. Thus, crystallization of 1D KNbO_3 nanostructures (generally unstable due to the natural tendency to form non-stoichiometric potassium niobates) was carried out through the reaction between Nb_2O_5 and KOH under H-MW preparation (Paula et al., 2008). The use of this method made possible a very fast preparation of single crystalline powders. Crystalline, single-phase, needle-like $\text{Ba}(\text{Mn}_{1/3}\text{Nb}_{2/3})\text{O}_3$ ceramics possessing high anisotropy were also described (Dias et al., 2009). Large crystals could be prepared from a direct combination of nanosized crystals under H-MW processing, which use leads to fast nucleation and production of nanosized particles, which could undergo a multiplying growth *via* a “cementing mechanism”. It was established that the Mn ions exhibit a particular role in the lattice dynamics in complex perovskites. BaMoO_4 powders were prepared by the coprecipitation method and processed in a domestic H-MW equipment (Cavalcante et al., 2008). It was shown that the BaMoO_4 powders present a polydisperse particle size distribution, are free of secondary phases and crystallize in a tetragonal structure. In another closely related research of the same authors, octahedron-like BaMoO_4 microcrystals were synthesized by the same method at room temperature and processed in H-MW equipment at 413 K for different times (from 30 min to 5 h) (Cavalcante et al., 2009). The researchers revealed that as-prepared BaMoO_4 microcrystals present an octahedron-like morphology with agglomerate nature and polydisperse particle size distribution. It was also indicated that the microcrystals grow along the [001] direction. A fast and economical route based on H-MW reaction was developed to synthesize pancake-like $\text{Fe}_2(\text{MoO}_4)_3$ microstructures (Zhang et al., 2010). It was established that several factors, including the amt. of nitric acid, reaction time, temperature and iron source, play crucial roles in the formation of the $\text{Fe}_2(\text{MoO}_4)_3$ multilayer stacked structures. The oriented attachment and layer-by-layer self-assembly of nanosheets is responsible for the formation of these structures. Additionally, micro-sized decaoctahedron BaZrO_3 powders (Fig. 8) were synthesized by means of a H-MW method at 140°C for 40 min (Moreira et al., 2009). A theoretical model derived from previous first principle calculations allowed authors to discuss the origin of the photoluminescence emission in BaZrO_3 powders which can be related to the local disorder in the network of both ZrO_6 octahedral and dodecahedral (BaO_{12}) hence forming the constituent polyhedron of BaZrO_3 system. The H-

MW processing was also employed to synthesize nanostructured alkaline-earth-metal (Ca, Ba, Sr) tungstate compounds in environmentally friendly conditions (110°C for times ranging from 5 to 20 min) (Siqueira et al., 2010).

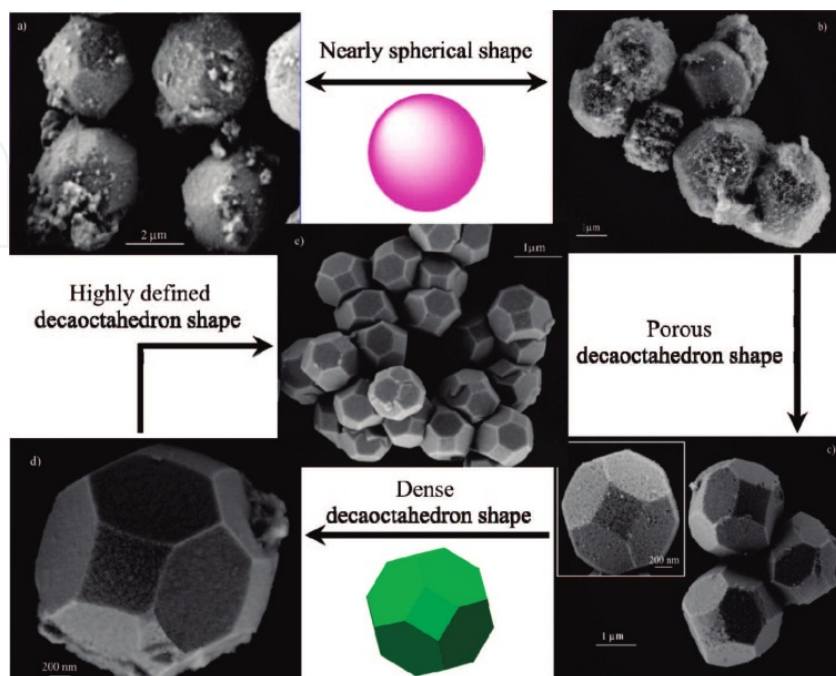


Figure 8. FE-SEM image of nearly spherical BaZrO₃ powders obtained for (a) 10 and (b) 20 min, and of decaoctahedral BaZrO₃ powders obtained for (c) 40, (d) 80, and (e) 160 min. With permission.

Ferrite salts, such as BiFeO₃ (Prado-Gonjal et al., 2009), and related compounds are common for H-MW synthesis. Thus, the pure phase of BiFeO₃ powder was synthesized by the H-MW method with FeCl₃·6H₂O and Bi(NO₃)₃·5H₂O powder as raw materials, KOH as mineralizer and Tween 80 as a surfactant (Zheng et al., 2011). It was indicated that the single phase of BiFeO₃ powder could be prepared *via* the H-MW method at 200°C for 1 h with KOH of 1.5 mol/L, the volume fraction of Tween 80 of 0–1.7% and a mole ratio of Fe to Bi of 1.0. When the hair ball-like BiFeO₃ powder was used as a catalyst, degradation rate of Rhodamine B increased from 48.92% to 79.71% after 4 h UV light irradiation. The formation of CoFe₂O₄ nanocrystals (particle size 6–11 nm) under hydrothermal conditions at 130°C was investigated (Kuznetsova et al., 2009). The hydrothermal medium was heated by 2 different methods, *i.e.*, the microwave (H-MW, with a reaction time from 1 min to 2 h) and conventional (with a time from 30 min to 45 h) methods. The use of microwave heating considerably accelerates the formation of CoFe₂O₄ particles. Preliminary ultrasonic treatment for 3 min increases the phase formation rate in the case of microwave heating and hardly affects the occurrence of the process upon conventional heating. In addition, (Ni_{0.30}Cu_{0.20}Zn_{0.50})Fe₂O_{4-x}MnO ($x = 0, 0.01, 0.02, 0.03, 0.04$) nanopowders were synthesized by H-MW method, and sintered into dense-ceramics under the conditions of 900°/4 h (Xu et al., 2007). It was established that Mn content can influence lattice parameters of samples; Mn-doping increases density of sintered Ni-Cu-Zn ferrites. Among other iron-containing compounds, we note nanocrystalline Yttrium Iron garnet (YIG) Y₃Fe₂(FeO₄)₃ with improved

magnetic properties (Sadhana et al., 2009) and tantalum oxide-added MgCuZn ferrite powders (Krishnaveni et al., 2006).

Other oxygen-containing salts are represented by a relatively small number of examples. Thus, by using H-MW crystallization approach, LiFePO_4 nanoparticles were synthesized in several minutes without the use of any organic reducing agent and argon protection (Yang, G. et al., 2011). A preferential orientation of crystal growth occurs upon MW hydrothermal field. The LiFePO_4 crystals present 1) a change from nanoparticle to nanosheet with the increasing reaction time from 5 to 20 min, 2) a couple of redox peaks in their CV profiles, whose pairs correspond to the charge/discharge reaction of the $\text{Fe}^{3+}/\text{Fe}^{2+}$ redox couple. The authors stated that, because of the LiFePO_4 samples prepared without any carbon, the initial charge/discharge capacities and cycleability of absolutely are affected by the crystal structure which is controlled by the MW irradiation condition. Flower-like PbGeO_3 microstructures were prepared at low temperature *via* H-MW solution-phase approach (Li, Z.-Q. et al., 2012). It was revealed that the entire structure of the architecture is composed of a large quantity of individual nanorods with 100-300 nm in width and several micrometers in length. Optical test showed that the absorption edge of the PbGeO_3 sample was 315 nm, corresponding to a bandgap of 3.94 eV. The CoAl_2O_4 pigment commonly used for coloring ceramic products was synthesized by the H-MW processing, and ink-jet printing with this aqueous pigment ink was performed to decorate porcelain (Obata et al., 2011). The synthesized CoAl_2O_4 particles were regular octahedrons measuring approximately 70 nm and were used to prepare an aqueous suspension, which was then used for printing on tiles by an ink-jet printing system. A convenient H-MW synthesis of nanostructured Cu^{2+} -substituted ZnGa_2O_4 spinels was reported (Conrad et al., 2010). A difference was observed in the coordination environments with Zn mostly situated on the tetrahedral sites of the spinel lattice whereas Cu is located on the octahedral sites of the nanostructured $\text{ZnGa}_2\text{O}_4:\text{Cu}^{2+}$ materials. Eu^{3+} , Dy^{3+} and Sm^{3+} doped nano-sized $\text{YP}_{0.8}\text{V}_{0.2}\text{O}_4$ phosphors were synthesized by a simple and facile microwave assisted hydrothermal process (Jin et al., 2011). Under UV excitation, the $\text{YP}_{0.8}\text{V}_{0.2}\text{O}_4:\text{Ln}^{3+}$ showed the VO_4^{3-} self-emission band at approximately 452 nm and the characteristic emission of doped lanthanide ions (Ln^{3+}). In addition, a facile H-MW route was developed to prepare oxynitride-based $(\text{Sr}_{1-x-y}\text{Ce}_x\text{Tb}_y)\text{Si}_2\text{O}_{2-\delta}\text{N}_{2+\mu}$ phosphors (Hsu & Lu, 2011). The emitting colors of the microwave-hydrothermally derived phosphors can be tuned over a wide range under UV excitation. Hectorite (white clay mineral) $\text{Na}_{0.4}\text{Mg}_{2.7}\text{Li}_{0.3}\text{Si}_4\text{O}_{10}(\text{OH})_2$ was prepared by aging the gel precursor by H-MW treatment at 393 K for 16 h (Vicente et al., 2009). Thus fabricated hectorite had higher purity (60%) than hectorite prepared by conventional heating (45%).

Sulfides, nitrides, and phosphides. To reduce the reaction time, electrical energy consumption, and cost, binary $\alpha\text{-NiS}$ - $\beta\text{-NiS}$ was synthesized by a H-MW within 15 min at temperatures of 160-180°C (Idris et al., 2011). At 140°C, pure hexagonal NiAs-type $\alpha\text{-NiS}$ phase was identified; with increasing reaction temperature (160-180°C), an increasing fraction of rhombohedral millerite-like $\beta\text{-NiS}$ is formed as a secondary phase. TEM imaging confirmed that needle-like protrusions connect the clusters of $\alpha\text{-NiS}$ particles.

Uniform nanorod and nanoplate structured Bi_2S_3 thin films were prepared on ITO substrates using a H-MW-assisted electrodeposition method (Wang et al., 2010). The obtained thin films are composed of orthorhombic phase Bi_2S_3 with good crystallinity. With the increase in the hydrothermal temperature (the best is 130°C), the crystallinity of the obtained films gradually improves and then decreases. In a related report (Thongtem et al., 2010), Bi_2S_3 nanorods in flower-shaped bundles were synthesized by decomposition of Bi-thiourea complexes under the microwave-assisted hydrothermal process. It was shown that Bi_2S_3 has the orthorhombic phase and appears as nanorods in flower-shaped bundles. Their UV-visible spectrum showed the absorbance at 596 nm, with its direct energy band gap of 1.82 eV. In addition, silver sulfide nanoworms (diameter of 50 nm and hundreds of nanometers in length) were prepared *via* a rapid H-MW by reacting silver nitrate and thioacetamide in the aqueous solution of the Bovine Serum Albumin (BSA) protein (Xing et al., 2011). It was shown that the nanoworms were assembled by multiple adjacent Ag_2S nanoparticles and stabilized by a layer of BSA attached to their surface. *In vitro* assays on the human cervical cancer cell line HeLa showed that the nanoworms exhibited good biocompatibility due to the presence of BSA coating. The authors stated that this combination of features makes the nanoworms attractive and promising building blocks for advanced materials and devices. As an example of practical application of metal calcogenides, obtained by H-MW technique, a red pigment, consisting of zirconium silicate-encapsulated particles of cadmium selenide sulfide, was prepared (Wang, F. et al., 2010). The GaN nanorods were synthesized by means of a combination of H-MW process and ammoniation at high temperature using Ga_2O_3 as raw material (Li, D. et al., 2011). It was found that GaN nanorods with aspect ratio of 5:1 are composed of highly oriented nanoparticles. The nanorods belong to hexagonal structure, whose crystal orientation is (002). The efficiencies of two methods of synthesizing InP micro-scale hollow spheres (Fig. 9) were compared (Xiuwen Zheng et al., 2009) *via* the analogous solution–liquid–solid (ASLS) growth mechanism, either through a traditional solvothermal procedure, or *via* a microwave-assisted method (S(H)-MW). $\text{InCl}_3 \cdot 4\text{H}_2\text{O}$, HAuCl_4 ethanol solution, P_4 and KBH_4 were used as precursors with ethylenediamine as solvent. MW synthesis was carried out for ca. 30 min under $180\text{--}220^\circ\text{C}$ at the microwave power 600 W. For traditional solvothermal route, long time (10 h) is necessary to obtain the micrometer hollow spheres, however, for the microwave-assisted route, 30 min is enough for hollow spherical products. Fig. 10 describes the formation mechanism of InP micro-scale hollow spheres, which, according to the authors, is as follows: under the thermal MW irradiation conditions, the reaction between P_4 molecules and In is on the surface of the In/Au droplets. Thereafter, the formed InP nanoparticles undergo the solidification to form compact InP layer on the surface of the Au/In core/shell droplets, which block the further reaction of P_4 with In molecules in the beads. As a result, when removing the unreacted In by diluted HCl solution, the inner Au cores separate from the outermost InP shells, and finally produce InP hollow spheres. Due to the loss of the support, some collapsed hollow spheres are formed.

Complex fluorides (Fig. 11) with well-defined cubic morphologies KMF_3 ($\text{M} = \text{Zn}, \text{Mn}, \text{Co}, \text{Fe}$, materials of technological importance, were synthesized (Kramer et al., 2008; Parhi et al.,

2008) from KF and MCl_2 ($M = Zn, Mn, Co, Fe$) in a Parr hydrothermal vessel, subjected to MW-heating in a domestic microwave operating for 4 min at 2.45 GHz with a maximum power of 1100 W, according to the reaction (6):

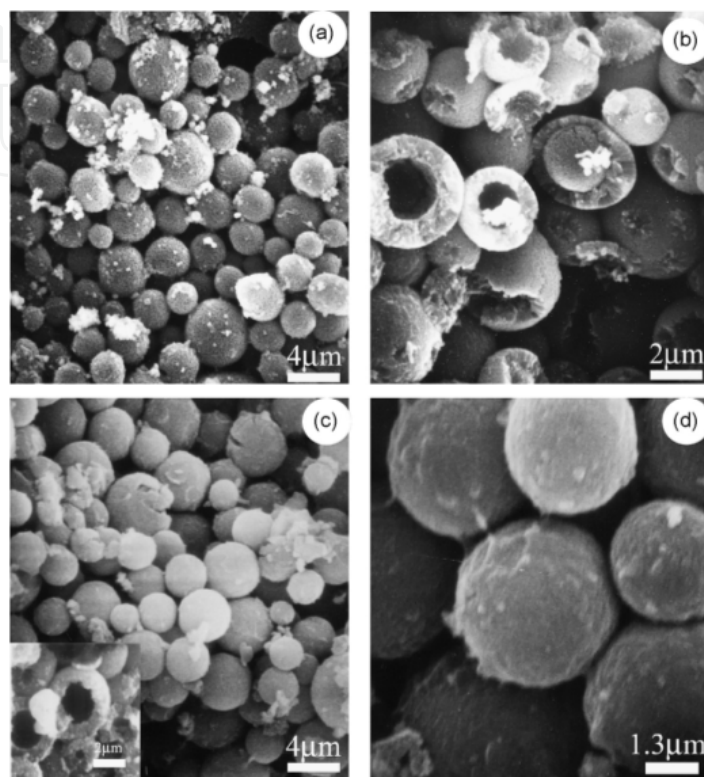
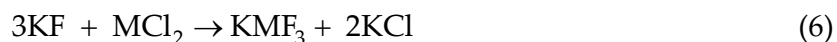


Figure 9. The SEM images (a and b) for T-InP (obtained by a **traditional** solvothermal procedure) samples and (c and d) for M-InP (obtained by a **microwave** solvothermal procedure) samples after HCl treatment. Inserted in (c) is the close-up of hollow nature for M-InP samples. With permission.

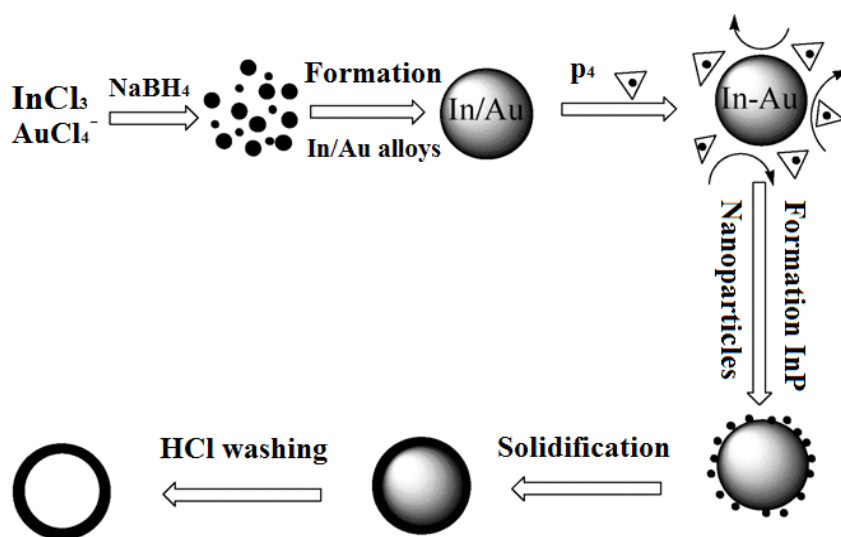


Figure 10. The proposed formation mechanism for InP hollow spheres. With permission.

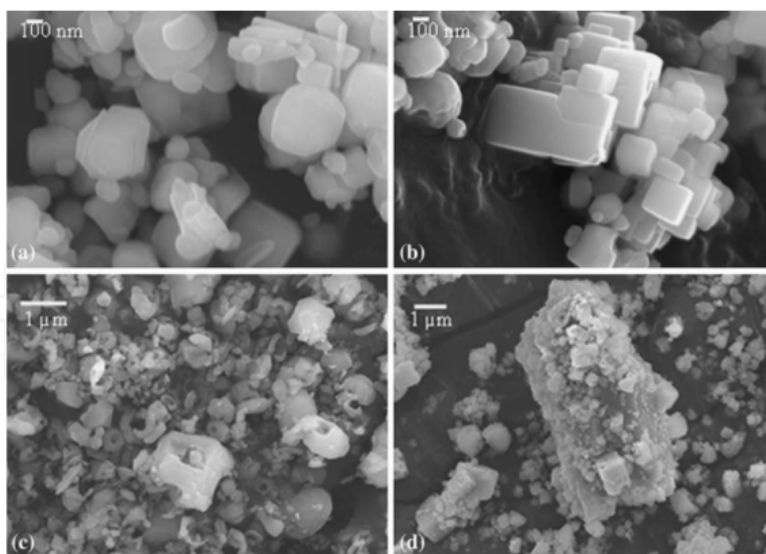


Figure 11. SEM images of (a) KZnF₃, (b) KMnF₃, (c) KCoF₃, and (d) KFeF₃ synthesized by H-MW method. With permission.

4. Composites

The composites, reported as fabricated by H-MW technique, are mainly based on the simple, double oxides or salts described above. Thus, transition metal oxide/graphene composites are known (Kim et al., 2011). For single-phase unitary/binary oxides-graphene composites, a two-step strategy to prepare them is as follows: precipitation of hydroxides followed by H(S)-MW annealing (Chang et al., 2010). This method was applied to the preparation of Mn₃O₄-graphene and NiCo₂O₄-graphene composites. Metal oxide / CNT nano-hybrid materials (LiMn₂O₄/CNT, LiCoO₂/CNT and Li₄Ti₅O₁₂/CNT nanocomposites) were synthesized through selective heterogeneous nucleation and growth of the oxides on CNT surface using H-MW process (Ma et al., 2010). In the composites, CNTs acted as a substrate to deposit nano-sized metal oxide and to connect the nanoparticles along 1D conduction path. The nano-hybrid materials showed excellent high rate capability and good structural reversibility for energy storage applications. H-MW synthesis method was also applied (Guo et al., 2009) for fabrication of tin dioxide nanoparticles-multiwalled carbon nanotubes (MWCNTs) composite powder for preparation of gas sensor. The mixed solution of SnCl₄·5H₂O and NaOH at mole ratio of 1:(8-12), NaCl and multiwalled carbon nanotubes (MWCNTs) were used as reactants, subjecting to ultrasonic dispersion, and reacting at 110-180°C for 30-300 min to synthesize SnO₂ nanoparticles-MWCNTs composite powder by microwave-assisted hydrothermal reaction. Se/C nanocomposite with core-shell structures was prepared through a facile one-pot H-MW process (Yu, J.C. et al., 2005). This material, consisting of a trigonal-Se (t-Se) core and an amorphous-C (a-C) shell, can be converted to hollow carbon capsules by thermal treatment. GaP nanocrystals/morin composite fluorescent materials were prepared by microwave hydrothermal synthesis method with Na₃P, GaCl₃ and morin as raw materials (Cui et al., 2001). It was shown that GaP nanocrystals underwent no structure transformation under the microwave hydrothermal condition, but they grew larger after the composite reaction with morin. The wavelength of

the composite materials blue-shifted and their luminescent efficiency increased when the particle size of GaP nanocrystals decreased.

Mesoporous composites of metal organic frameworks (MOFs; Cu-based) with boehmite and silica were prepared by one-pot H-MW synthesis in the presence of Pluronic-type triblock-copolymer (Gorka et al., 2010). Mesoporosity in these composites can be tailored by varying the MOF/oxide phase ratio. Fe-JLU-15 materials with different Si/Fe ratios (Si/Fe = 90, 50, 10) were synthesized by H-MW process (Bachari et al., 2009). These species correspond to hematite particles, very small "isolated" or oligomeric Fe(III) species possibly incorporated in the mesoporous silica wall, and Fe(III) oxide clusters either isolated or agglomerated, forming "rafts" at the surface of the silica and exhibiting ferromagnetic ordering. Applying similar Fe-FSM-16 materials, the liquid-phase benzylation of aromatic compounds with benzyl chloride (BC) was investigated (Bachari et al., 2010). Catalytic data in the benzylation of aromatic compounds such as benzene and toluene with BC show that Fe-FSM-16 samples synthesized by the M-H process are very active and recyclable catalysts. Nano-TiO₂ and super fine Al₂O₃ composite powder was developed by H-MW method, and TiO₂-Al₂O₃ semiconductor-dielectric composite ceramics with uniform fine grain structure were prepared by fast speed sintering in H₂ atmosphere (Lu & Zhang, 2003). Titania-hydroxyapatite (TiO₂-HAp) nanocomposite was produced by H-MW technique (Pushpakanth et al., 2008); but, in case of related Ca, Sr and Ca_{0.5}Sr_{0.5} hydroxyapatites (Komarneni, Noh et al., 2010), microwave-assisted reactions did not lead to accelerated syntheses of hydroxyapatites in comparison with conventional-hydrothermal method, because the crystallization of these materials occurred at very low temperature.

In addition, the nano-sized BaTiO₃ and NiCuZn ferrite powders (40-60 nm) were synthesized at 160°C for 45 min (Sadhana, Praveena et al., 2009). These $x\text{BaTiO}_3 + (1-x)\text{NiCuZnFe}_2\text{O}_4$ nano-composites were prepared at different weight percentages. It was observed that these composites were useful for the fabrication of Multilayer Chip Inductors (MLCI). The related nanocomposites of NiCuZnFe₂O₄-SiO₂ (particle size of 20 nm) were prepared using H-MW method in the same conditions (Praveena et al., 2010). Among a little of organic matter-containing composites, we note the synthesis of poly (3,4-ethylenedioxythiophene)/V₂O₅ (PEDOT/V₂O₅) by *in-situ* oxidation of monomer (3,4-ethylenedioxythiophene) into crystalline nanostrip V₂O₅ using H-MW technique (Ragupathy et al., 2011). It was observed that the interlayer spacing of V₂O₅ upon intercalation of the polymer expands from 4.3 to 14°.

5. Ceramics

The hydrothermal synthesis of oxidic ceramic powders was reviewed (Somiya et al., 2005) for the decomposition of complex oxides like ilmenite, the hydrothermal oxidation of metals, hydrothermal precipitation, combinations of electrochemical, mechanical, microwave and sonochemical methods with hydrothermal methods. Niobates are widely described as ceramic basis. Thus, using KNN ("kalium" (potassium) nitrate niobate) powder

prepared by the H-MW method as raw material, traditional ceramic method was employed to fabricate the KNN based lead-free piezoelectric ceramic with 1 mol.% ZnO or 1 mol.% CuO sintering additives (Li, Y. et al., 2011). The preparation method of lithium-doped potassium sodium niobate-based lead-free piezoelectric ceramic powder was based on use of MOH (M=Li, Na, K) and Nb₂O₅ as raw materials in a H-MW reactor (Tan et al., 2011). The advantages of the offered technique were low reaction temperature, short reaction period, high reaction activity of obtained powder, low energy consumption, and environmental friendliness. In addition, K_{0.5}Na_{0.5}NbO₃ lead-free piezoelectric ceramics were prepared from their powders which were synthesized by H-MW method (Zhou et al., 2010). The results indicated that phase of KNN ceramics were pure orthorhombic symmetry. When the powders synthesized at 160°C for 7 h, the final ceramic grains possess considerably better distribution and more homogenous in size.

Among other ceramics, indium vanadates for severe applications as photocatalysts, anodes for Li rechargeable batteries or electrochromic devices were prepared *via* H-MW synthesis performed at 220°C for different reaction times (Bartonickova et al., 2010). The H-MW method was applied to the preparation of strontium-doped lanthanum manganites with different stoichiometric ratio of the three oxides, La_{1-x}Sr_xMnO₃ ($x = 0.3, 0.5, 0.6$) (Rizzuti & Leonelli, 2009). The complete chemistry, mineralogical and microstructural characterization of the powders revealed the same structural properties of the perovskite powders previously synthesized by ceramic and conventional hydrothermal routes. In addition, a series of Ni_{0.5-x}Cu_xZn_{0.5}Fe₂O₄ ($x = 0.05, 0.10, 0.15, \text{ and } 0.20$) ferrites nanopowders were synthesized by H-MW method, and sintered into dense-ceramics under the conditions of 900°C/4 h (Zheng, Ya-lin et al., 2007). The performed studies showed within a limited Cu content range of $x = 0.05\text{--}0.20$, copper ions were present in different ionic states in the A- and B-sites which could influence the size of lattice parameter. It was also found that crystallite size, initial permeability, resistivity and quality factor were the highest when the Cu content was 0.20.

6. Metal complexes

There are obviously no many examples of coordination compounds, obtained by H(S)-MW technique due to low stability of organic matter in hydrothermal conditions. Thus, an organic-inorganic UV absorber [Hgua]₂(Ti₅O₅F₁₂) was obtained (Lhoste et al., 2011), whose 3D network is built up from infinite inorganic layers ∞(Ti₅O₅F₁₂) separated by guanidinium cations. Under UV irradiation at 254 nm for 40 h, the white microcrystalline powder turned to light purple-gray due to reduction of Ti(IV) to Ti(III), confirmed by magnetic measurements. Two extended solids displaying both 1D coordination polymer [Co(H₂O)₄(4,4'-bipy)](4,4'-bipyH₂)₂(SO₄)₂·2H₂O (bipy = 2,2'-bipyridine) and 2D H-bonded structural features [Co₂(4,4'-bipy)₂(SO₄)₂(H₂O)₆]₄(H₂O) were prepared (Prior et al., 2011) under H-MW conditions. Within the first framework is located a twice protonated 4,4'-bipyridine molecule (C₁₀N₂H₁₀²⁺) which forms 2 short N-H·····O H-bonds and 8 further non-classical C-H·····O interactions. The second compound displays 1D chains of Co-bipyridine which are sinusoidal in nature. Three mixed-ligand Co(II) complexes (Shi et al., 2009)

$[\text{Na}_2\text{Co}(\mu_4\text{-btec})(\text{H}_2\text{O})_8]_n$, $[\text{Co}_2(\mu_2\text{-btec})(\text{bipy})_2(\text{H}_2\text{O})_6]\cdot 2\text{H}_2\text{O}$, and $[\text{Co}_2(\mu_2\text{-btec})(\text{phen})_2(\text{H}_2\text{O})_6]\cdot 2\text{H}_2\text{O}$ (H_4btec = 1,2,4,5-benzenetetracarboxylic acid, phen = 1,10-phenanthroline) are also known. A vanadium 2,6-naphthalenedicarboxylate, $\text{V}^{\text{III}}(\text{OH})(\text{O}_2\text{C-C}_{10}\text{H}_6\text{-CO}_2)\cdot \text{H}_2\text{O}$ was synthesized under S-MW procedure (Liu, Y.-Ya et al., 2012). After calcination at 250°C in air, the V^{III} center was oxidized to V^{IV} with the structure of $\text{V}^{\text{IV}}\text{O}(\text{O}_2\text{C-C}_{10}\text{H}_6\text{-CO}_2)$. The last compound, in the liquid-phase oxidation of cyclohexene, exhibited catalytic performance similar to $[\text{VO}(\text{O}_2\text{C-C}_6\text{H}_4\text{-CO}_2)]$. The compound is reusable and maintains its catalytic activity through several runs. Purinium, adeninium, and guaninium fluoroaluminates, $[\text{Hpur}]_2(\text{AlF}_5)$, $[\text{Hade}]_3(\text{AlF}_6)\cdot 6.5\text{H}_2\text{O}$ and $[\text{Hguan}]_3(\text{Al}_3\text{F}_{12})$, were synthesized by H-MW synthesis at 120°C or 190°C (Cadiou et al., 2011). Authors commented that the crystallization was difficult; all crystals of the first two complexes were very small while only a microcrystalline powder of the third compound was obtained. The purine, adenine, and guanine amines were found to be monoprotonated and lie between the preceding chains or layers.

By treating $\text{Cu}(\text{NO}_3)_2\cdot 3\text{H}_2\text{O}$ with a V-shaped ligand 4,4'-oxydibenzoic acid (H_2oba), a dynamic metal-carboxylate framework $[\text{Cu}_2(\text{oba})_2(\text{DMF})_2]\cdot 5.25\text{DMF}$ (MCF-23, Fig. 12) was synthesized, which features a wavelike layer with rhombic grids based on the paddle-wheel secondary building units (Xiao-Feng Wang et al., 2008). MCF-23 synthesized by conventional solvothermal methods always contained considerable and intractable impurities. In contrast, a S-MW method was proven to be a faster and greener approach to synthesize phase-pure MCF-23 in high yield. Larger crystals suitable for single-crystal diffraction could be obtained by the multistep microwave heating mode. Also, a 3D coordination copper polymer, $[\text{Cu}_2(\text{pyz})_2(\text{SO}_4)(\text{H}_2\text{O})_2]_n$ (pyz = pyrazine), was synthesized under H-MW conditions (Amo-Ochoa et al., 2007). The authors especially note that microwave assisted synthesis produces monocystal suitable for X-ray diffraction studies, reducing reaction time and with higher yield than the classical hydrothermal procedures.

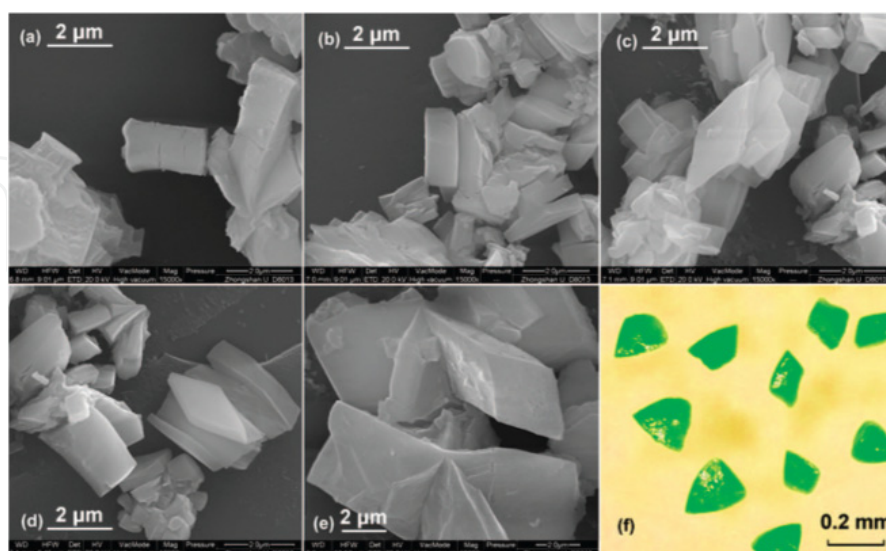


Figure 12. SEM images of MCF-23 synthesized *via* single-step microwave-assisted solvothermal synthesis (MASS): (a) 1 min, (b) 5 min, (c) 10 min, (d) 30 min, (e) 150 min at 160°C , and (f) photo of single crystals synthesized *via* multistep MASS. With permission.

Single crystals of $[\text{H}_3\text{dien}]\cdot(\text{FeF}_6)\cdot\text{H}_2\text{O}$ and $[\text{H}_3\text{dien}]\cdot(\text{CrF}_6)\cdot\text{H}_2\text{O}$ were obtained by S-MW (Ben Ali et al., 2007). These structures are built up from isolated FeF_6 or CrF_6 octahedra, water molecules and triprotonated amines; each octahedron is connected by hydrogen bonds to six organic cations and two water molecules. ^{57}Fe Mossbauer spectrometry proved the hyperfine structure confirming the presence of Fe^{3+} in octahedral coordination and reveals the existence of paramagnetic spin fluctuations. Under H-MW conditions, two compounds $\text{Zn}(\text{pinH})(\text{H}_2\text{O})$ and $\text{Cd}(\text{pinH})$ were obtained through the reactions of Zn (or Cd) sulfate and 2-phosphonic-isonicotinic acid (pinH_3) (Yang Yi-F. et al., 2007). The authors established that the first complex has a layer structure in which double chains composed of corner-sharing $\{\text{ZnO}_5\text{N}\}$ octahedra and $\{\text{CPO}_3\}$ tetrahedra are cross-linked through the carboxylate groups. The latter has a framework structure where the inorganic layers composed of edge-sharing $\{\text{CdO}_5\text{N}\}$ octahedra and $\{\text{CPO}_3\}$ tetrahedra are pillared by the pyridyl carboxylate groups. A 3D open-framework and a chain-structured zinc terephthalate were obtained by hydrothermal crystallization under microwave heating at 180°C (Rajic et al., 2006). These structures have rather similar principal building units, which facilitates the structure transformation from the low-dimensional to the open-framework one during crystallization. For the optimization of the H-MW synthesis of $[\text{Zn}(\text{BDC})(\text{H}_2\text{O})_2]_n$, where H_2BDC = 1,4-benzenedicarboxylic acid, the reactions were carried out at the fixed temperature of 120°C for 10, 20, 30 and 40 min (Wanderley et al., 2011). Pure crystalline $[\text{Zn}(\text{BDC})(\text{H}_2\text{O})_2]_n$ was obtained in high yield (90%) with a reaction time of 10 min.

7. Other materials and processes

Series of reports are devoted to H-MW fabrication of a variety of *molecular sieves* and other *adsorbents*. Thus, a range of nanosize alkaline-free gallosilicate mesoporous molecular sieves (GaMMS) were synthesized using H-MW method (Cheng et al., 2011). These nanosize GaMMSs exhibited high surface area ($240\text{--}720\text{ m}^2/\text{g}$), pore volume ($1.06\text{--}1.49\text{ m}^3/\text{g}$), narrow pore size distribution and nano-particle size between 20 and 100 nm and four-coordinated gallium site mainly. It was revealed that the nanosize GaMMS shows a much higher activity than that of conventional GaMCM-41, probably due to higher concentrations of H-form sites, external surface and fast diffusion. Mesoporous molecular sieves MCM-41 modified by single (Ti) and bimetal (Ti-V) ions with highly ordered hexagonal arrangement of their cylindrical channels were prepared by direct synthesis under H-MW conditions at 403 K (Guo, Y. et al., 2010). It was shown that Ti and V ions were introduced into MCM-41 under M-H conditions and Ti/V-Si bond was formed. The modified materials were high active and selective in the epoxidation of styrene at 343 K in comparison with single functional MCM-41. The applied method greatly improved the selectivity to styrene oxide. In addition, a rapid process to prepare cryptomelane-type octahedral molecular sieve (OMS-2) nanomaterials using a H-MW technique (MW-HT) for 10 s (in comparison with up to 4 days in a conventional hydrothermal reaction) was presented (Huang, H. et al., 2010). It was shown that the OMS-2 nanowires were produced from thin nano-flakes with increasing reaction temperatures. Carbon/silica adsorbents (carbosils) were prepared by pyrolysis of CH_2Cl_2 at 823 K and the reaction time from 0.5 to 6 h on the mesoporous silica gel surface

and then hydrothermally treated at 473 K with steam or liquid water by using the classical autoclave with traditional heating way or in the microwave reactor (Skubiszewska-Zieba, 2008). It was stated that hydrothermal treatment in the microwave reactor, contrary to that in the classical autoclave, allowed obtaining adsorbents with noticeably higher values of total pore volume in relation to the initial adsorbents and in majority with a higher specific surface area. Application of microwave energy allowed obtaining adsorbents with lower values of surface free energy in relation to the initial adsorbents and those modified in the autoclave.

Carbon-based materials are also produced by H-MW method. Thus, rice chaff can be converted into activated carbon by alkaline treatment at high temperature, in particular by H-MW treatment with NaOH solution (Inada et al., 2011). Rice chaff was heated at 700°C for 1 h in N₂ after HCl treatment to remove impurity, such as alkali metals, resulting in the formation of charcoal. After further necessary steps, it was revealed that the specific surface area of product was 1060 m²/g under microwave irradiation and 690 m²/g by conventional heating with autoclave, which indicated that H-MW treatment is effective for activation of charcoal. In addition, acidic suspensions of multi-walled carbon nanotubes (MWCNTs) in 5 M HNO₃ solutions were readily obtained by microwave-assisted hydrothermal digestion and their rapid surface functionalization with polyaniline could be achieved growing composite coatings *in situ* onto graphite electrodes in an acidified suspension of MWCNTs and aniline (Wu et al., 2007). The advantage of the integrity of the MWCNTs after microwave exposure was used to improve the mechanical strength of the composite coatings, especially when an utmost thick coating was attempted for a high capacitance.

Materials and processes using iron-containing compounds. Iron-FSM [folded-sheet mesoporous material]-16 materials with different Si/Fe ratio (Si/Fe = 90, 60, and 10) were synthesized by H-MW process (Bachari et al., 2011). These species correspond to hematite particles, small isolated Fe(III) species possibly incorporated in the mesoporous silica wall, and iron oxide clusters either isolated or agglomerated, forming rafts at the surface of the silica and exhibiting ferromagnetic ordering. It was shown that Fe-FSM-16 synthesized this way are active and recycle catalysts. The high yield and rapid precipitation of Fe(III) arsenate(V) dihydrate (identical to the mineral scorodite) from aqueous Fe(III)-As(V) solutions at pH 0.6-1.1 was achieved long ago using microwave dielectric heating (Baghurst et al., 1995). The process could be useful for As removal from industrial wastes. Metallic iron (α -Fe)/manganese-zinc ferrite (Fe_{3-x-y}Mn_xZn_yO₄) nanocomposites were synthesized for 15 s using H(S)-MW treatment of alcohol solutions of chloride precursors and sodium ethoxide (Caillot et al., 2011). For all samples, 20% of metallic iron was routinely obtained using the microwave flash synthesis. Consequently, the microwave heating appears to provide an efficient source of energy in producing metallic iron nanoparticles protected against oxidation by an oxide matrix. Additionally, as an improvement of the conventional hydrothermal reaction with iron powder, NaOH and H₂O as reactants at 423 K, leading to iron oxide Fe₃O₄, NaFeO₂ and hydrogen, MW-heating was adopted to induce the hydrothermal reaction (Liu, X. et al., 2011). Under MWs, NaOH and H₂O absorbed microwave energy by space charge polarization and dipolar polarization and instantly

converted it into thermal energy, which initiated the hydrothermal reaction that involved with zero-valent iron. The developed microwave-hydrothermal reaction was employed for the dechlorination of PCBs (polychlorinated biphenyls). For PCBs in 10 mL simulative transformer oil, almost complete dechlorination was achieved by 750 W MW irradiation for 10 min, with 0.3 g iron powder, 0.3 g NaOH and 0.6 mL H₂O added. The authors stated that MW irradiation combined with the common and cheap materials, iron powder, NaOH and H₂O, might provide a fast and cost-effective method for the treatment of PCBs-containing wastes.

Zeolites/alumosilicates, composites and membranes on their basis are frequently (especially ZSM-5) obtained by the discussed method. Thus, evaluation of hydrothermal synthesis of the zeolite BZSM-5 was performed by treating the synthesis mixture by different aging processes, namely, ultrasonic, static, stirring, and microwave-assisted aging prior to the conventional hydrothermal treatment (Abrishamkar et al., 2010). That the ultrasonic and microwave assisted aging shortened the crystallization time and altered the crystal size and the morphology of the obtained products. Mullite (Al₆Si₂O₁₃) powders were prepared by sol-gel combined with H-MW process using tetra-Et orthosilicate and Al(NO₃)₃·9H₂O as raw materials (Yang, Q. et al., 2010). It was shown that the increasing of microwave hydrothermal temperature can decrease the synthetic temperature of mullite. The initial temperature of the mullitization of gels was about 1046°C, but the temperature of preparation of pure mullite should be at 1300°C, which can be decreased to 1200°C through H-MW process. Using silatrane and alumatrane templates, remarkably uniform zeolites (NaA, EDI-type, ABW-type, FAU-type, K, and ZSM-5 zeolites) were obtained via the sol-gel process and H-MW treatment to obtain small and uniform zeolite crystals to prepare zeolite membranes (Wongkasemjit, 2009). The organic ligands of both precursors not only make the molecules stable to moisture, but also, after hydrolysis, provide trialkanolamine molecules which could function as another template for the reaction. The formation of ZSM-5 zeolite/porous carbon composite from carbonized rice husk was investigated using microwave- and conventional-hydrothermal reaction at 140-160°C (Katsuki et al., 2005). It was established that, compared to the conventional-hydrothermal (C-H) formation of ZSM-5 zeolite, the H-MW reaction led to increased rate of formation by 3-4 times at 150°C. The surface area of ZSM-5 zeolite (without template)/porous carbon composite was shown to be 485.4 m²/g and this composite had both micropores and mesopores. Zeolite nanocrystals (e.g., silicalite-1, ZSM-5, LTL, BEA and LTA) with controllable size, morphology and SiO₂/Al₂O₃ ratio were prepared (Yuan Yuan Hu et al., 2009). It is found that high synthesis temperature and long reaction time benefit the growth of all the referred zeolite nanocrystals. The authors established that for the nanozeolites crystallized in low alkalinity systems (e.g., ZSM-5, BEA and LTA), both increasing the alkalinity and decreasing the water content accelerate their nucleation process and thereby result in the decrease of their crystal size. On the contrary, for those prepared in high alkalinity systems (e.g., LTL and silicalite-1), an inversed trend could be observed. In addition, stable zeolite beta coatings with a thickness of 1-2 μm were synthesized on a borosilicate glass substrate by H-MW synthesis (Muraza et al., 2008). In addition, a regular nanocrystalline supramolecular Mg-Al hydrotalcite was prepared *via* glycol-frequency H-MW reaction using MgCl₂·6H₂O,

$\text{AlCl}_3 \cdot 6\text{H}_2\text{O}$ as raw material and Na_2CO_3 as precipitator (Wu, J. et al., 2010). It was shown that the hydroxalite exhibited as a homogeneous and hexagonal sheet.

A high quality pure hydroxy-sodalite $\text{Na}_8[\text{AlSiO}_4]_6(\text{OH})_2$ zeolite membrane was H-MW-synthesized on an $\alpha\text{-Al}_2\text{O}_3$ support (Xiaochun Xu et al., 2004). This process only needed 45 min and synthesis was more than 8 times faster than by the conventional hydrothermal synthesis method. The pure hydroxy-sodalite zeolite membrane method was found to be well inter-grown and the thickness of the membrane was 6–7 μm . Gas permeation results showed that the hydrogen/n-butane permselectivity of the hydroxy-sodalite zeolite membrane was larger than 1000, being a promising candidate for the separation of hydrogen from gas mixtures and important for the emerging hydrogen energy fuel system. The potential of microwave heating for the rapid synthesis of thin silicalite-1 membranes by secondary growth from microwave-derived silicalite-1 seeds was evaluated (Motuzas et al. 2006). The morphology, thickness, homogeneity, crystal preferential orientation and single gas permeation properties of the silicalite-1 membranes were studied in relation to the synthesis parameters. Other related zeolite-ceramic membranes (titanosilicalite TS-1 (Sebastian, V.; Motuzas, J. et al., 2010) and MFI-type (Sebastian, V.; Mallada, R. et al., 2010)) are also known.

Other H-MW-synthesized materials and compounds are rare; some of them also found useful practical applications, as, for example, titanium-based nanometer pigments (Paskocimas et al., 2009). CdS/Titanate nanotubes (TNTs) were also prepared (Chen, Y.-C. et al., 2011). It was established that the CdS nanoparticles synthesized using a 140-W microwave irradiation power at 423 K photodegraded 26% ammonia in water, while the photocatalytic efficiency increased to 52.3% using the synthesized CdS/TNTs composites. So, it can be stated that the CdS/TNTs photocatalysts possess improved photocatalytic activity than that of CdS or TNTs materials alone. Mesoporous composites of metal organic frameworks (MOFs; Cu-based) with boehmite and silica were prepared by one-pot H-MW synthesis in the presence of Pluronic-type triblock-copolymer (Gorka, J.; Fulvio, P.F. et al., 2010). A variety of visible-light-driven silver vanadates, including $\alpha\text{-AgVO}_3$, $\beta\text{-AgVO}_3$, and $\alpha\text{-Ag}_3\text{VO}_4$, were synthesized using a H-MW synthesis method (Pan et al., 2011). The $\alpha\text{-Ag}_3\text{VO}_4$ crystalline sample with rich hydroxyl functional groups on the surface exhibited the highest degree of photocatalytic activity. Thus, the reaction rates of the photodegradation of isopropanol (IPA) and benzene vapors were approximately 8 times higher than those of P25 under visible-light irradiation. In addition, the photocatalytic activities of H-MW samples were higher than those of samples produced by conventional hydrothermal techniques. The authors explained this due to an increase in the specific surface area and additional hydroxyl functional groups on the surface. Another application of the H-MW method for destruction of organic pollutants was reported in (Liu, X. et al., 2011). The reaction of reduced iron powder and NaOH or KOH led to obtaining iron oxides and/or ferrites, releasing hydrogen for quick dechlorination of persistent organic pollutants. The method was shown to have the advantages of short treatment time and high dechlorination efficiency and can be used for treating waste organochlorine pesticides, polychlorobiphenyl oil in transformer, soil and sediment heavily polluted by organochlorine pesticides and

polychlorobiphenyl oil, and garbage burning fly ash and chlor-alkali brine sludge containing high-concentration dioxins. $\text{Ca}(\text{OH})_2$ alone and $\text{Ca}(\text{OH})_2$ with H_3PO_4 addition (P-addition) were effectively used to remove and recover boron from wastewater using hydrothermal methods (Tsai et al., 2011). A microwave hydrothermal method was also used and compared with the conventional heating method in batch experiments. For the case of $\text{Ca}(\text{OH})_2$ alone and the MW method, experimental results showed that boron recovery efficiency reached 90% within 10 min, and crystals of $\text{Ca}_2\text{B}_2\text{O}_5 \cdot \text{H}_2\text{O}$ were observed. For the case of P-addition and the MW method, boron recovery efficiency reached 99% within 10 min, and Ca phosphate species ($\text{CaHPO}_4 \cdot \text{H}_2\text{O}$, CaHPO_4 and $\text{Ca}_{10}(\text{PO}_4)_6(\text{OH})_2$) were formed. Hydrophobic organoclays (hybrids derived from an ion exchange of hydrophilic clays with quaternary ammonium salts and used as rheological additives in paints, inks, cosmetics, nanocomposites, and as pollutant absorbing agents in soil remediation programs) were studied using a natural (Na-montmorillonite) and several synthetic clays (Na-fluorophlogopites) as precursors (Baldassari). These organoclays synthesized using both conventional hydrothermal and H-MW processes.

8. Conclusions

Nowadays, the H(S)-MW techniques are already classic method for fabrication of distinct chemical compounds and materials, including nanomaterials. Inorganic compounds and materials are generally obtained by this route, although a certain number of organic-containing compounds are also reported. Use of organic matter in this method can be considered as a careful pioneer experimentation in order to check its suitability for MW-hydro(solvo)thermal reactions. Compounds, which are stable in hydrothermal conditions, such as metal oxides, oxygen-containing and other metal salts, a variety of zeolites, carbon-based materials, as well as composites on their basis, are classic synthesis objects by this route. It is expected that more organic/organometallic products could be tried to be prepared in H(S)-MW conditions, for example thermally stable (up to 500-600°C, that is rare for organic matter) aromatic macrocycles of phthalocyanine (Edrissi et al., 2007) type and related compounds.

Author details

Boris I. Kharisov, Oxana V. Kharissova and Ubaldo Ortiz Méndez
Universidad Autónoma de Nuevo León, Monterrey, México

9. References

- Abrishamkar, M.; Azizi, S.N.; Kazemian, H. (2010). Ultrasonic-Assistance and Aging Time Effects on the Zeolitization Process of BZSM-5 Zeolite. *Zeitschrift fuer Anorganische und Allgemeine Chemie*, 636(15), 2686-2690.
- Al-Tuwirqi, R.M.; Al-Ghamdi, A.A.; Al-Hazmi, F.; Alnowaiser, F.; Al-Ghamdi, A.A.; Aal, N.A.; El-Tantawy, F. (2011). Synthesis and physical properties of mixed $\text{Co}_3\text{O}_4/\text{CoO}$

- nanorods by microwave hydrothermal technique. *Superlattices and Microstructures*, 50(5), 437-448.
- Amo-Ochoa, P.; Givaja, G.; Miguel, P.J.S; Castillo, O.; Zamora, F. (2007). Microwave assisted hydrothermal synthesis of a novel CuI-sulfate-pyrazine MOF. *Inorganic Chemistry Communications*, 10(8), 921-924.
- Bachari, K.; Lamouchi, M. (2009). Synthesis and Characterization of Fe-JLU-15 Mesoporous Silica Via a Microwave-Hydrothermal Process. *Journal of Cluster Science*, 20(3), 573-586.
- Bachari, K.; Guerroudj, R. M.; Lamouchi, M. (2011). High activities of iron-FSM-16 materials synthesized by a microwave-hydrothermal process in Friedel-Crafts alkylations. *Kinetics and Catalysis*, 52(1), 119-127.
- Bachari, K.; Guerroudj, R. M.; Lamouchi, M. (2010). Catalytic performance of iron-mesoporous nanomaterials synthesized by a microwave-hydrothermal process. *Reaction Kinetics, Mechanisms and Catalysis*, 100(1), 205-215.
- Baghurst, D.R.; Barrett, J.; Mingos, D.M.P. (1995). The hydrothermal microwave synthesis of scorodite: iron(III) arsenate(V) dihydrate, $\text{FeAsO}_4 \cdot 2\text{H}_2\text{O}$. *Journal of the Chemical Society, Chemical Communications*, (3), 323-324.
- Baldassari, S.; Komarneni, S.; Mariani, E.; Villa, C. (2006). Microwave versus conventional preparation of organoclays from natural and synthetic clays. *Applied Clay Science*, 31(1-2), 134-141.
- Bartonickova, E.; Cihlar, J. (2010). Synthesis and processing of InVO_4 ceramics. *International Journal of Modern Physics B: Condensed Matter Physics, Statistical Physics, Applied Physics*, 24(6&7), 770-779.
- Belousov, O.V.; Belousova, N.V.; Sirotina, A.V.; Solovyov, L.A.; Zhyzhaev, A.M.; Zharkov, S.M.; Mikhlin, Y.L. (2011). Formation of Bimetallic Au-Pd and Au-Pt Nanoparticles under Hydrothermal Conditions and Microwave Irradiation. *Langmuir*, 27(18), 11697-11703.
- Ben Ali, A.; Dang, M.T.; Greneche, J.-M.; Hemon-Ribaud, A.; Leblanc, M.; Maisonneuve, V. (2007). Synthesis, structure of $[\text{H}_3\text{dien}](\text{MF}_6) \cdot \text{H}_2\text{O}$ ($\text{M} = \text{Cr}, \text{Fe}$) and ^{57}Fe Moessbauer study of $[\text{H}_3\text{dien}](\text{FeF}_6) \cdot \text{H}_2\text{O}$. *Journal of Solid State Chemistry*, 180(6), 1911-1917.
- Cadiau, A.; Adil, K.; Hemon-Ribaud, A.; Leblanc, M.; Jouanneaux, A.; Slawin, A. M. Z.; Lightfoot, P.; Maisonneuve, V. (2011). Fluoroaluminates of purine and DNA bases, adenine, guanine. $[\text{Hpur}]_2(\text{AlF}_5)$, $[\text{Hade}]_3(\text{AlF}_6) \cdot 6.5\text{H}_2\text{O}$, $[\text{Hguan}]_3(\text{Al}_3\text{F}_{12})$. *Solid State Sciences*, 13(1), 151-157.
- Caillot, T.; Pourroy, G.; Stuerge, D. (2011). Novel metallic iron/manganese-zinc ferrite nanocomposites prepared by microwave hydrothermal flash synthesis. *Journal of Alloys and Compounds*, 509(8), 3493-3496.
- Cao, C.-Y.; Cui, Z.-M.; Chen, C.-Q.; Song, W.-G.; Cai, W. (2010). Ceria Hollow Nanospheres Produced by a Template-Free Microwave-Assisted Hydrothermal Method for Heavy Metal Ion Removal and Catalysis. *Journal of Physical Chemistry C*, 114(21), 9865-9870.
- Cavalcante, L. S.; Sczancoski, J. C.; Tranquilin, R. L.; Joya, M. R.; Pizani, P. S.; Varela, J. A.; Longo, E. (2008). BaMoO_4 powders processed in domestic microwave-hydrothermal:

- Synthesis, characterization and photoluminescence at room temperature. *Journal of Physics and Chemistry of Solids*, 69(11), 2674-2680.
- Cavalcante, L.S.; Sczancoski, J.C.; Tranquilin, R.L.; Varela, J.A.; Longo, E.; Orlandi, M.O. (2009). Growth mechanism of octahedron-like BaMoO₄ microcrystals processed in microwave-hydrothermal: experimental observations and computational modeling. *Particuology*, 7(5), 53-362.
- Chang, K.-H.; Lee, Y.-F.; Hu, C.-C.; Chang, C.-I.; Liu, C.-L.; Yang, Yi-L. (2010). A unique strategy for preparing single-phase unitary/binary oxides-graphene composites. *Chemical Communications*, 46(42), 7957-7959.
- Chen, J.; Luo, K. (2008). Synthesis of Ba_{0.75}Sr_{0.25}Zr_{0.1}Ti_{0.9}O₃ nano-powder by microwave-hydrothermal method. *Taoci* (Xianyang, China), (10), 28-30.
- Chen, Y.-C.; Lo, S.-L.; Ou, H.-H.; Chen, C.-H. (2011). Photocatalytic oxidation of ammonia by cadmium sulfide/titanate nanotubes synthesized by microwave hydrothermal method. *Water Science and Technology*, 63(3), 550-557.
- Chen, Z.; Li, W.; Zeng, W.; Li, M.; Xiang, J.; Zhou, Z.; Huang, J. (2008). Microwave hydrothermal synthesis of nanocrystalline rutile. *Materials Letters*, 62(28), 4343-4344.
- Cheng, C.-F.; Liu, S.-M.; Cheng, H.-H.; Yao, M.G.; Liu, S.B. (2011). Microwave hydrothermal synthesis and acidity of nanosize gallosilicate mesoporous molecular sieves. *Journal of the Chinese Chemical Society*, 58(2), 155-162.
- Conrad, F.; Zhou, Y.; Yulikov, M.; Hametner, K.; Weyeneth, S.; Jeschke, G.; Guenther, D.; Grunwaldt, J.-D.; Patzke, G.R. (2010). Microwave-Hydrothermal Synthesis of Nanostructured Zinc-Copper Gallates. *European Journal of Inorganic Chemistry*, (13), 2036-2043.
- Cui, D.; Wei, J.; Pan, J.; Hao, X.; Xu, X.; Jiang, M. (2001). Preparation and characterization of GaP nano-composite fluorescent material. *Gongneng Cailiao*, 32(5), 543-545.
- Dias, A.; Matinaga, F.M.; Moreira, R.L. (2009). Vibrational Spectroscopy and Electron-Phonon Interactions in Microwave-Hydrothermal Synthesized Ba(Mn_{1/3}Nb_{2/3})O₃ Complex Perovskites. *Journal of Physical Chemistry B*, 113(29), 9749-9755.
- Dos Santos, M. L.; Lima, R. C.; Riccardi, C. S.; Tranquilin, R. L.; Bueno, P. R.; Varela, J. A.; Longo, E. (2008). Preparation and characterization of ceria nanospheres by microwave-hydrothermal method. *Materials Letters*, 62(30), 4509-4511.
- Edrissi, M.; Nasernejad, B.; Sayedi, B. (2007). Novel method for the preparation of copper phthalocyanine blue nanoparticles in an electrochemical cell irradiated by microwave. *IJE Transactions B: Applications*, 20(3), 257-262.
- Elizari, S.A.; Cavalcante, L.S.; Sczancoski, J.C.; Pizani, A.P.C.; Varela, J.A.; Espinosa, J.W.M.; Longo, E. (2009). Morphology and Photoluminescence of HfO₂ Obtained by Microwave-Hydrothermal. *Nanoscale Res. Lett.*, 4, 1371-1379.
- Gorka, J.; Fulvio, P.F.; Pikus, S.; Jaroniec, M. (2010). Mesoporous metal organic framework-boehmite and silica composites. *Chemical Communications*, 46(36), 6798-6800.
- Gorka, J.; Fulvio, P.F.; Pikus, S.; Jaroniec, M. (2010). Mesoporous metal organic framework-boehmite and silica composites. *Chemical Communications*, 46(36), 6798-6800.

- Guiotoku, M.; Maia, C. M. B. F.; Rambo, C.R.; Hotza, D. (2011). Chapter 13. Synthesis of Carbon-Based Materials by Microwave Hydrothermal Processing. in *"Microwave Heating"*, Edited By: Usha Chandra, INTECH, pp. 291-308.
- Guo, M.; Wang, Y.; Zhang, M.; Wang, X.; Yue, C. (2009). Microwave-assisted hydrothermal synthesis method for tin dioxide nanoparticles-multiwalled carbon nanotubes (MWCNTs) composite powder for preparation of gas sensor. 7 pp., CN 101439855.
- Guo, Y.; Wang, G.; Wang, Y.; Liu, Z.; Liu, G.; Liu, Y. (2010). Microwave hydrothermal synthesis of bimetallic (Ti-V) ions modified MCM-41 for epoxidation of styrene. *Materials Research Society Symposium Proceedings*, 1279(New Catalytic Materials), Paper #26.
- Hariharan, V.; Parthibavarman, M.; Sekar, C. (2011). Synthesis of tungsten oxide ($W_{18}O_{49}$) nanosheets utilizing EDTA salt by microwave irradiation method. *Journal of Alloys and Compounds*, 509(14), 4788-4792.
- Hsu, C.-H.; Lu, C.-H. (2011). Microwave-hydrothermally synthesized $(Sr_{1-x-y}Ce_xTb_y)Si_2O_7$ phosphors: efficient energy transfer, structural refinement and photoluminescence properties. *Journal of Materials Chemistry*, 21(9), 2932-2939.
- Huang, C.-H.; Yang, Y.-T.; Doong, R.-A. (2011). Microwave-assisted hydrothermal synthesis of mesoporous anatase TiO_2 via sol-gel process for dye-sensitized solar cells. *Microporous and Mesoporous Materials*, 142(2-3), 473-480.
- Idris, N.H.; Rahman, Md.M.; Chou, S.-L.; Wang, J.-Z.; Wexler, D.; Liu, H.-K. (2011). Rapid synthesis of binary α -NiS- β -NiS by microwave autoclave for rechargeable lithium batteries. *Electrochimica Acta*, 58, 456-462.
- Inada, M.; Koga, T.; Tanaka, Y.; Enomoto, N.; Hojo, J. (2011). Synthesis of activated carbon from rice chaff by microwave hydrothermal method. *Funtai oyobi Funmatsu Yakin*, 58(10), 598-601.
- Ivanov, V.K.; Polezhaeva, O.S.; Gil', D.O.; Kopitsa, G.P.; Tret'yakov, Yu.D. (2009). Hydrothermal Microwave Synthesis of Nanocrystalline Cerium Dioxide. *Doklady Chemistry*, 426(2), 131-133.
- Jia, J.; Yu, J.C.; Wang, Yi-X.J.; Chan, K.M. (2010). Magnetic Nanochains of $FeNi_3$ Prepared by a Template-Free Microwave-Hydrothermal Method. *ACS Applied Materials & Interfaces*, 2(9), 2579-2584.
- Jin, Yu; Li, C.; Xu, Z.; Cheng, Z.; Wang, W.; Li, G.; Lin, J. (2011). Microwave-assisted hydrothermal synthesis and multicolor tuning luminescence of $YPr_xV_{1-x}O_4:Ln^{3+}$ ($Ln = Eu, Dy, Sm$) nanoparticles. *Materials Chemistry and Physics*, 129(1-2), 418-423.
- Huang, H.; Sithambaram, S.; Suib, S. (2010). Microwave-assisted hydrothermal synthesis of cryptomelane-type octahedral molecular sieves (OMS-2) and their catalytic studies. Abstracts of Papers, 240th ACS National Meeting, Boston, MA, United States, August 22-26, 2010, CATL-48.
- Huang, J.; Xia, C.; Cao, L.; Zeng, X. (2008). Facile microwave hydrothermal synthesis of zinc oxide one-dimensional nanostructure with three-dimensional morphology. *Materials Science and Engineering B*, 150, 187-193.

- Katsuki, H.; Furuta, S.; Watari, T.; Komarneni, S. (2005). ZSM-5 zeolite/porous carbon composite: Conventional- and microwave-hydrothermal synthesis from carbonized rice husk. *Microporous and Mesoporous Materials*, 86(1-3), 145-151.
- Katsuki, H. (2009). Sintering of α -Fe₂O₃ particles prepared from microwave-hydrothermal reaction. *Funtai oyobi Funmatsu Yakin*, 56(12), 738-743.
- Kim, G.B.; Kim, H.G.; Kim, Ji.Y.; Park, S.H. (2011). Preparation method of transition metal oxide/graphene composite using microwave-hydrothermal process and its use in energy-storage devices and gas sensors. 17 pp., KR 2011121584.
- Koga, N.; Kimizu, T. (2008). Thermal decomposition of indium(III) hydroxide prepared by the microwave-assisted hydrothermal method. *Journal of the American Ceramic Society*, 91(12), 4052-4058.
- Komarneni, S.R.; Pidugu, Quing Hua Li; Roy, R. (1995). Microwave-hydrothermal processing of metal powders. *J. Mater. Res.*, 10(7), 1687-1692.
- Komarneni, S.; Hussein, M. Z.; Liu, C.; Breval, E.; Malla, P. B. (1995). Microwave-hydrothermal processing of metal clusters supported in and/or on montmorillonite. *European Journal of Solid State and Inorganic Chemistry*, 32(7/8), 837-849.
- Komarneni, S. (2003). Nanophase materials by hydrothermal, microwave-hydrothermal, and microwave-solvothermal methods. *Current Science*, 85(12), 1730-1734.
- Komarneni, S.; Katsuki, H. (2002). Nanophase materials by a novel microwavehydrothermal process. *Pure Appl. Chem.*, 74(9), 1537-1543.
- Komarneni, S.; Katsuki, H. (2010). Microwave-hydrothermal synthesis of barium titanate under stirring condition. *Ceramics International*, 36(3), 1165-1169.
- Komarneni, S.; Noh, Y.D.; Kim, J.Y.; Kim, S.H.; Katsuki, H. (2010). Solvothermal/hydrothermal synthesis of metal oxides and metal powders with and without microwaves. *Zeitschrift fuer Naturforschung, B: A Journal of Chemical Sciences*, 65(8), 1033-1037.
- Kramer, J.W.; Parhi, P.; Manivannan, V. (2008). Microwave Initiated Hydrothermal Synthesis of Nano-Sized Complex Fluorides, KMF₃ (Zn, Mn, Co and Fe). Abstracts, 43rd Midwest Regional Meeting of the American Chemical Society, Kearney, NE, United States, October 8-11, 2008, MWRM-319.
- Krishna, M.; Komarneni, S. (2009). Conventional- vs microwave-hydrothermal synthesis of tin oxide, SnO₂ nanoparticles. *Ceramics International*, 35(8), 3375-3379.
- Krishnaveni, T.; Murthy, S. R.; Gao, F.; Lu, Q.; Komarneni, S. (2006). Microwave hydrothermal synthesis of nanosize Ta₂O₅ added Mg-Cu-Zn ferrites. *Journal of Materials Science*, 41(5), 1471-1474.
- Kuznetsova, V. A.; Almjasheva, O. V.; Gusarov, V. V. (2009). Influence of microwave and ultrasonic treatment on the formation of CoFe₂O₄ under hydrothermal conditions. *Glass Physics and Chemistry*, 35(2), 205-209.
- Lhoste, J.; Rocquefelte, X.; Adil, K.; Dessapt, R.; Jobic, S.; Leblanc, M.; Maisonneuve, V.; Bujoli-Doeuff, M. (2011). A New Organic-Inorganic Hybrid Oxyfluorotitanate [Hgua]₂(Ti₅O₅F₁₂) as a Transparent UV Filter. *Inorganic Chemistry*, 50(12), 5671-5678.

- Li, C.; Yu, R.; Ren, T.; Zhang, W. (2011). Microwave hydrothermal-deposition synthesis method for directional nanobar-structured ZnO thin film. 13 pp. CN 102260046.
- Li, D.; Wang, F.; Zhu, J.-f.; Xue, X.-s. (2011). Synthesis and characterization of GaN nanorods by microwave hydrothermal method and treatment with ammonia. *Gongneng Cailiao Yu Qijian Xuebao*, 17(2), 218-222.
- Li, J.; Huang, J.; Yu, C.; Wu, J.; Cao, L.; Yanagisawa, K. (2011). Hierarchically structured snowflakelike $\text{WO}_3 \cdot 0.33\text{H}_2\text{O}$ particles prepared by a facile, green, and microwave-assisted method. *Chemistry Letters*, 40(6), 579-581.
- Li, W.-h. (2008). Microwave-assisted hydrothermal synthesis and optical property of Co_3O_4 nanorods. *Materials Letters*, 62(25), 4149-4151.
- Li, Z.-Q.; Zhang, L.; Lin, X.-S.; Chen, X.-T.; Xue, Zi-L. (2012). Fast preparation of flower-like PbGeO_3 microstructures at low-temperature via a microwave-assisted hydrothermal process. *Materials Letters*, 68, 344-346.
- Li, Y.; Liu, H.; Shen, Z.; Hong, Y.; Wang, Z.; Li, R. (2011). Effect of ZnO and CuO sintering additives on the properties of KNN piezoelectric ceramic. *Zhongguo Taoci*, 47(10), 28-31.
- Liu, X.; Zhao, W.; Zhang, G.; Sun, K.; Zhao, Y. (2011). Method for treating persistent organic pollutants through microwave hydrothermal reaction. 6 pp., CN 102068782.
- Liu, Y.-Ya; Leus, K.; Grzywa, M.; Weinberger, D.; Strubbe, K.; Vrielinck, H.; Van Deun, R.; Volkmer, D.; Van Speybroeck, V.; Van Der Voort, P. (2012). Synthesis, Structural Characterization, and Catalytic Performance of a Vanadium-Based Metal-Organic Framework (COMOC-3). *European Journal of Inorganic Chemistry*, Ahead of Print <http://onlinelibrary.wiley.com/doi/10.1002/ejic.201101099/abstract>
- Liu, H.; He, X.-m.; Li, G.-j.; Cai, Zi-j.; Zhu, Z.-f. (2011). Microwave hydrothermal synthesis of AlOOH and Al_2O_3 hierarchically nanostructured microspheres self-assembled by nanosheets. *Gongneng Cailiao*, 42(5), 854-857, 861.
- Liu, X.; Zhao, W.; Sun, K.; Zhang, G.; Zhao, Y. (2011). Dechlorination of PCBs in the simulative transformer oil by microwave-hydrothermal reaction with zero-valent iron involved. *Chemosphere*, 82(5), 773-777.
- Lu, Y.; Zhang, J. (2003). Development of $\text{TiO}_2\text{-Al}_2\text{O}_3$ semiconductor-dielectric composite ceramics and investigation on its microwave-absorbing properties. *Xiyou Jinshu Cailiao Yu Gongcheng*, 32(Suppl. 1), 463-466.
- Lv, Y.; Liu, Y.; Dai, S.; Shi, S. (2009). Synthesis of $\text{Bi}_{0.5}\text{Na}_{0.5}\text{TiO}_3$ spherical particles by microwave hydrothermal process. 7 pp., CN 101525239.
- Ma, S.B.; Kim, J.G.; Kim, H.-K.; Choi, H.-R.; Kim, K.-B. (2010). Metal oxide/carbon nanotubes nano-hybrid materials for energy storage applications. Abstracts of Papers, 240th ACS National Meeting, Boston, MA, United States, August 22-26, 2010, FUEL-52.
- Maksimov, V. D.; Meskin, P. E.; Churagulov, B. R. (2008). Hydrothermal microwave synthesis of finely divided powders of simple and complex zirconium and hafnium oxides. *Poverkhnost*, (2), 76-82.
- Moreira, M.L.; Andres, J.; Varela, J.A.; Longo, E. (2009). Synthesis of Fine Micro-sized BaZrO_3 Powders Based on a Decaohedron Shape by the Microwave-Assisted Hydrothermal Method. *Crystal Growth & Design*, 9(2), 833-839.

- Morishima, Y.; Kobayashi, M.; Petrykin, V.; Kakihana, M.; Tomita, K. (2007). Microwave-assisted hydrothermal synthesis of brookite nanoparticles from a water-soluble titanium complex and their photocatalytic activity. *Journal of the Ceramic Society of Japan*, 115(Dec.), 826-830.
- Motuzas, J.; Julbe, A.; Noble, R. D.; van der Lee, A.; Beresnevicius, Z. (2006). Rapid synthesis of oriented silicalite-1 membranes by microwave-assisted hydrothermal treatment. *J. Microporous and Mesoporous Materials*, 92(1-3), 259-269.
- de Moura, A. P.; Lima, R. C.; Moreira, M. L.; Volanti, D. P.; Espinosa, J. W. M.; Orlandi, M. O.; Pizani, P. S.; Varela, J. A.; Longo, E. (2010). ZnO architectures synthesized by a microwave-assisted hydrothermal method and their photoluminescence properties. *Solid State Ionics*, 181(15-16), 775-780.
- de Moura, A. P.; Lima, R. C.; Paris, E. C.; Li, M. S.; Varela, J. A.; Longo, E. (2011). Formation of nickel hydroxide plate-like structures under mild conditions and their optical properties. *Journal of Solid State Chemistry*, 184(10), 2818-2823.
- Muraza, O.; Rebrov, E.V.; Chen, J.; Putkonen, M.; Niinistö, L.; de Croon, M.H.J. M.; Schouten, J.C. (2008). Microwave-assisted hydrothermal synthesis of zeolite Beta coatings on ALD-modified borosilicate glass for application in microstructured reactors. *Chemical Engineering Journal*, 135(Suppl. 1), S117-S120.
- Nyutu, E.K.; Chun-Hu Che; Dutta, P.K.; Suib, S.L. (2008). Effect of Microwave Frequency on Hydrothermal Synthesis of Nanocrystalline Tetragonal Barium Titanate. *J. Phys. Chem. C*, 112, 9659-9667.
- Obata, S.; Kato, M.; Yokoyama, H.; Iwata, Y.; Kikumoto, M.; Sakurada, O. (2011). Synthesis of nano CoAl_2O_4 pigment for ink-jet printing to decorate porcelain. *Journal of the Ceramic Society of Japan*, 119(Mar.), 208-213.
- Pan, G.-T.; Lai, M.-H.; Juang, R.-C.; Chung, T.-W.; Yang, T.C.-K. (2011). Preparation of Visible-Light-Driven Silver Vanadates by a Microwave-Assisted Hydrothermal Method for the Photodegradation of Volatile Organic Vapors. *Industrial & Engineering Chemistry Research*, 50(5), 2807-2814.
- Parhi, P.; Kramer, J.; Manivannan, V. (2008). Microwave initiated hydrothermal synthesis of nano-sized complex fluorides, KMF_3 ($\text{M} = \text{Zn}, \text{Mn}, \text{Co}, \text{and Fe}$). *Journal of Materials Science*, 43(16), 5540-5545.
- Paskocimas, C.A.; Longo da Silva, E.; Volanti, D.P.; Varela, J.A.; Silva Junior, W.; Silva, W.; Boeing, E. (2009). Process for preparation of titanium-based nanometer pigments by hydrothermic preparation aided with microwaves. *Braz. Patente PI*, 19 pp., BR 2008001228.
- Paula, A.J.; Parra, R.; Zaghete, M.A.; Varela, J.A. (2008). Synthesis of KNbO_3 nanostructures by a microwave assisted hydrothermal method. *Materials Letters*, 62(17-18), 2581-2584.
- Pires, F. I.; Joanni, E.; Savu, R.; Zaghete, M. A.; Longo, E.; Varela, J. A. (2008). Microwave-assisted hydrothermal synthesis of nanocrystalline SnO powders. *Materials Letters*, 62(2), 239-242.

- Prado-Gonjal, J.; Villafuerte-Castrejon, M. E.; Fuentes, L.; Moran, E. (2009). Microwave-hydrothermal synthesis of the multiferroic BiFeO₃. *Materials Research Bulletin*, 44(8), 1734-1737.
- Praveena, K.; Sadhana, K.; Murthy, S.R. (2010). Microwave-hydrothermal synthesis of Ni_{0.53}Cu_{0.12}Zn_{0.35}Fe₂O₄/SiO₂ nanocomposites for MLCI. *Integrated Ferroelectrics*, 119, 122-134.
- Prior, T.J.; Yotnoi, B.; Rujiwatra, A. (2011). Microwave synthesis and crystal structures of two cobalt-4,4'-bipyridine-sulfate frameworks constructed from 1-D coordination polymers linked by hydrogen bonding. *Polyhedron*, 30(2), 259-268.
- Pushpakanth, S.; Srinivasan, B.; Sreedhar, B.; Sastry, T.P. (2008). An *in situ* approach to prepare nanorods of titania-hydroxyapatite (TiO₂-HAp) nanocomposite by microwave hydrothermal technique. *Materials Chemistry and Physics*, 107(2-3), 492-498.
- Ragupathy, P.; Vasan, H.N.; Munichandraiah, N.; Vasanthacharya, N. (2011). *In-situ* preparation of PEDOT/V₂O₅ nanocomposite and its synergism for enhanced capacitive behavior. *Proceedings of SPIE*, 8035 (Energy Harvesting and Storage: Materials, Devices, and Applications II), 80350I/1-80350I/11.
- Rajic, N.; Stojakovic, D.; Logar, N. Zabukovec; Kaucic, V. (2006). An evidence for a chain to network transformation during the microwave hydrothermal crystallization of an open-framework zinc terephthalate. *Journal of Porous Materials*, 13(2), 153-156.
- Rizzuti, A.; Leonelli, C. (2009). Microwave advantages in inorganic synthesis of La_{0.5}Sr_{0.5}MnO₃ powders for perovskite ceramics. *Processing and Application of Ceramics*, 3(1-2), 29-32.
- Sadhana, K.; Shinde, R.S.; Murthy, S.R. (2009). Synthesis of nanocrystalline YIG using microwave-hydrothermal method. *International Journal of Modern Physics B: Condensed Matter Physics, Statistical Physics, Applied Physics*, 23(17), 3637-3642.
- Sadhana, K.; Praveena, K.; Bharadwaj, S.; Murthy, S.R. (2009). Microwave-Hydrothermal synthesis of BaTiO₃+NiCuZnFe₂O₄ nanocomposites. *Journal of Alloys and Compounds*, 472(1-2), 484-488.
- Sczancoski, J.C.; Cavalcante, L.S.; Joya, M.R.; Varela, J.A.; Pizani, P.S.; Longo, E. (2008). SrMoO₄ powders processed in microwave-hydrothermal: Synthesis, characterization and optical properties. *Chemical Engineering Journal*, 140, 632-637.
- Sebastian, V.; Mallada, R.; Coronas, J.; Julbe, A.; Terpstra, R.A.; Dirrix, R.W.J. (2010). Microwave-assisted hydrothermal rapid synthesis of capillary MFI-type zeolite-ceramic membranes for pervaporation application. *Journal of Membrane Science*, 355(1-2), 28-35.
- Sebastian, V.; Motuzas, J.; Dirrix, R.W.J.; Terpstra, R.A.; Mallada, R.; Julbe, A. (2010). Synthesis of capillary titanosilicalite TS-1 ceramic membranes by MW-assisted hydrothermal heating for pervaporation application. *Separation and Purification Technology*, 75(3), 249-256.
- Shangzhao Shi; Jiann-Yang Hwang. (2003). Microwave-assisted wet chemical synthesis: advantages, significance, and steps to industrialization. *Journal of Minerals & Materials Characterization & Engineering*, 2(2), 101-110.

- Shi, Z.-F.; Jin, J.; Li, L.; Xing, Y.-H.; Niu, S.-Y. (2009). Syntheses, structures, and surface photoelectric properties of Co-btec complexes. *Wuli Huaxue Xuebao*, 25(10), 2011-2019.
- Shojaee, N.; Ebadzadeh, T.; Aghaei, A. (2010). Effect of concentration and heating conditions on microwave-assisted hydrothermal synthesis of ZnO nanorods. *Materials Characterization*, 61(12), 1418-1423.
- Sikhwivhilu, L.M.; Mpelane, S.; Moloto, N.; Ray, S.S. (2010). Hydrothermal synthesis of TiO₂ nanotubes: microwave heating versus conventional heating. *Ceramic Engineering and Science Proceedings*, 31(7, Nanostructured Materials and Nanotechnology IV), 45-49.
- Simoës, A. Z.; Moura, F.; Onofre, T. B.; Ramirez, M. A.; Varela, J. A.; Longo, E. (2010). Microwave-hydrothermal synthesis of barium strontium titanate nanoparticles. *Journal of Alloys and Compounds*, 508(2), 620-624.
- Siqueira, K.P.F.; Moreira, R.L.; Valadares, M.; Dias, A. (2010). Microwave-hydrothermal preparation of alkaline-earth-metal tungstates. *Journal of Materials Science*, 45(22), 6083-6093.
- Skubiszewska-Zieba, J. (2008). Structural and energetic properties of carbosils hydrothermally treated in the classical autoclave or the microwave reactor. *Adsorption*, 14(4/5), 695-709.
- Somiya, S.; Roy, R.; Komarneni, S. (2005). Hydrothermal synthesis of ceramic oxide powders. *Materials Engineering*, 28(Chemical Processing of Ceramics (2nd Edition)), 3-20.
- Suchanek, W.L.; Riman, R.E. (2006). Hydrothermal Synthesis of Advanced Ceramic Powders. *Advances in Science and Technology*, 45, 184-193.
- Sun, M.; Li, D.; Zhang, W.; Fu, X.; Shao, Y.; Li, W.; Xiao, G.; He, Y. (2010). Rapid microwave hydrothermal synthesis of GaOOH nanorods with photocatalytic activity toward aromatic compounds. *Nanotechnology*, 21(35), 355601/1-355601/7.
- Sun, Q.; Luo, J.; Xie, Z.; Wang, J.; Su, X. (2008). Synthesis of monodisperse WO₃·2H₂O nanospheres by microwave hydrothermal process with (+)-tartaric acid as a protective agent. *Materials Letters*, 62(17-18), 2992-2994.
- Sun, W.; Pang, Y.; Li, J.; Ao, W. (2007). Particle Coarsening II: Growth Kinetics of Hydrothermal BaTiO₃. *Chemistry of Materials*, 19(7), 1772-1779.
- Tan, G.; Xiong, P.; Qin, B. (2011). Method for preparing lithium-doped potassium sodium niobate-based lead-free piezoelectric ceramic powder by microwave hydrothermal method. 7 pp., CN 102205988.
- Tapala, S.; Thammajak, N.; Laorattanakul, P.; Rujiwatra, A. (2008). Effects of microwave heating on sonocatalyzed hydrothermal preparation of lead titanate nanopowders. *Materials Letters*, 62(21-22), 3685-3687.
- Thongtem, T.; Pilapong, C.; Kavinchan, J.; Phuruangrat, A.; Thongtem, S. (2010). Microwave-assisted hydrothermal synthesis of Bi₂S₃ nanorods in flower-shaped bundles. *Journal of Alloys and Compounds*, 500(2), 195-199.
- Tsai, H.-C.; Lo, S.-L. (2011). Boron removal and recovery from concentrated wastewater using a microwave hydrothermal method. *Journal of Hazardous Materials*, 186(2-3), 1431-1437.

- Vicente, I.; Salagre, P.; Cesteros, Y.; Guirado, F.; Medina, F.; Sueiras, J.E. (2009). Fast microwave synthesis of hectorite. *Applied Clay Science*, 43(1), 103-107.
- Volanti, D.P.; Orlandi, M.O.; Andres, J.; Longo, E. (2010). Efficient microwave-assisted hydrothermal synthesis of CuO sea urchin-like architectures via a mesoscale self-assembly. *Cryst. Eng. Comm.*, 12(6), 1696-1699.
- Wanderley, K.A.; Alves, S., Jr.; Paiva-Santos, C. de Oliveira. (2011). Microwave-assisted hydrothermal synthesis as an efficient method for obtaining $[\text{Zn}(\text{BDC})(\text{H}_2\text{O})_2]_n$ metal-organic framework. *Quimica Nova*, 34(3), 434-438.
- Wang, F.; Liu, D.; Li, Q.; Li, D.; Zhu, J. (2010). Method for preparation of red pigment consisting of zirconium silicate-encapsulated particles of cadmium selenide sulfide by microwave hydrothermal process. 9 pp., CN 101786902.
- Wang, L.; Li, B.; Yang, M.; Chen, C.; Liu, Y. (2011). Effect of Ni cations and microwave hydrothermal treatment on the related properties of layered double hydroxide-ethylene vinyl acetate copolymer composites. *Journal of Colloid and Interface Science*, 356(2), 519-525.
- Wang, Y.; Huang, J.-F.; Zhu, H.; Cao, Li-Y.; Xue, X.-S.; Zeng, X.-R. (2010). Preparation of Bi_2S_3 thin films by microwave-hydrothermal assisted electrodeposition method. *Wuji Huaxue Xuebao*, 26(6), 977-981.
- Wei, G.; Qin, W.; Zhang, D.; Wang, G.; Kim, R.; Zheng, K.; Wang, L. (2009). Synthesis and field emission of MoO_3 nanoflowers by a microwave hydrothermal route. *Journal of Alloys and Compounds*, 481(1-2), 417-421.
- Wongkasemjit, S. (2009). Novel route to remarkably uniform zeolites. Editor(s): Wongkasemjit, S.; Jamieson, A.M. *Advanced Metal and Metal Oxide Technology*, 1-18. Publisher: Transworld Research Network, Trivandrum, India.
- Wu, J.; Liang, H.; Xiao, Y.; Lin, J. (2010). Glycol-frequency microwave-hydrothermal synthesis and characterization of excellent quality Mg-Al hydrotalcite. *Zhongshan Daxue Xuebao, Ziran Kexueban*, 49(3), 70-74.
- Wu, M.; Zhang, L.; Wang, D.; Gao, J.; Zhang, S. (2007). Electrochemical capacitance of MWCNT/polyaniline composite coatings grown in acidic MWCNT suspensions by microwave-assisted hydrothermal digestion. *Nanotechnology*, 18(38), 385603/1-385603/7.
- Xiao-Feng Wang; Yue-Biao Zhang; Hong Huang; Jie-Peng Zhang; Xiao-Ming Chen. (2008). Microwave-Assisted Solvothermal Synthesis of a Dynamic Porous Metal-Carboxylate Framework. *Cryst. Growth & Design*, 8(12), 4559-4563.
- Xiaochun Xu; Yun Bao; Chunshan Song; Weishen Yang; Jie Liu; Liwu Lin. (2004). Microwave-assisted hydrothermal synthesis of hydroxy-sodalite zeolite membrane. *Microporous and Mesoporous Materials*, 75, 173-181.
- Xie, Y.; Yin, S.; Hashimoto, T.; Kimura, H.; Sato, T. (2009). Microwave-hydrothermal synthesis of nano-sized Sn^{2+} -doped BaTiO_3 powders and dielectric properties of corresponding ceramics obtained by spark plasma sintering method. *Journal of Materials Science*, 44(18), 4834-4839.

- Xing, R.; Liu, S.; Tian, S. (2011). Microwave-assisted hydrothermal synthesis of biocompatible silver sulfide nanoworms. *Journal of Nanoparticle Research*, 13(10), 4847-4854.
- Xiuwen Zheng; Qitu Hua; Chuansheng Sun. (2009). Efficient rapid microwave-assisted route to synthesize InP micrometer. *Mater. Res. Sci.*, 44(1), 216-219.
- Xu, G.-l.; Zheng, Ya-l.; Lai, Z.-yu. (2007). Effects of Mn on the properties of Ni-Cu-Zn ferrites. *Xinan Keji Daxue Xuebao*, 22(4), 10-13, 19.
- Yang, G.; Ji, H.; Miao, X.; Hong, A.; Yan, Y. (2011). Crystal growth behavior of LiFePO_4 in microwave-assisted hydrothermal condition: from nanoparticle to nanosheet. *Journal of Nanoscience and Nanotechnology*, 11(6), 4781-4792.
- Yang, Q.; Huang, J.-f.; Cao, Li-y.; Wang, B.; Wu, J.-p.; Yang, T. (2010). Preparation of mullite microcrystallites by sol-gel combined with microwave hydrothermal process. *Rengong Jingti Xuebao*, 39(6), 1456-1460.
- Yang, Yi-F.; Ma, Y.-S.; Bao, S.-S.; Zheng, Li-M. (2007). Microwave-assisted hydrothermal syntheses of metal phosphonates with layered and framework structures. *Dalton Transactions*, (37), 4222-4226.
- Yang, Yi-Lin; Hu, Chi-Chang; Hua, Chi-Chung. (2011). Preparation and characterization of nanocrystalline $\text{Ti}_x\text{Sn}_{1-x}\text{O}_2$ solid solutions via a microwave-assisted hydrothermal synthesis process. *Cryst. Eng. Comm.*, 13(19), 5638-5641.
- Yuanyuan Hu; Chong Liu; Yahong Zhang; Nan Ren; Yi Tang. (2009). Microwave-assisted hydrothermal synthesis of nanozeolites with controllable size. *Microporous and Mesoporous Materials*, 119, 306-314.
- Yoon, S.; Manthiram, A. (2011). Microwave-hydrothermal synthesis of $\text{W}_{0.4}\text{Mo}_{0.6}\text{O}_3$ and carbon-decorated $\text{WO}_x\text{-MoO}_2$ nanorod anodes for lithium ion batteries. *Journal of Materials Chemistry*, 21(12), 4082-4085.
- Yu, J.C.; Hu Xianluo; Li Quan; Zheng Zhi; Xu Yeming. (2005). Synthesis and characterization of core-shell selenium/carbon colloids and hollow carbon capsules. *Chemistry*, 12(2), 548-52.
- Yu, Y.-T.; Dutta, P. (2011). Synthesis of Au/SnO_2 core-shell structure nanoparticles by a microwave-assisted method and their optical properties. *Journal of Solid State Chemistry*, 184(2), 312-316.
- Zawadzki, M. (2008). Microwave-assisted synthesis and characterization of ultrafine neodymium oxide particles. *Journal of Alloys and Compounds*, 451(1-2), 297-300.
- Zeng, R.; Wang, J.-Q.; Chen, Z.-X.; Li, W.-X.; Dou, S.-X. (2011). The effects of size and orientation on magnetic properties and exchange bias in Co_3O_4 mesoporous nanowires. *Journal of Applied Physics*, 109(7), 07B520/1-07B520/3.
- Zhang, L.; Cao, X.-F.; Ma, Y.-Li; Chen, X.-T.; Xue, Zi-L. (2010). Pancake-like $\text{Fe}_2(\text{MoO}_4)_3$ microstructures: microwave-assisted hydrothermal synthesis, magnetic and photocatalytic properties. *New Journal of Chemistry*, 34(9), 2027-2033.
- Zhao, Q.; Yang, Y.; Sun, Y.-x.; Wang, S.-g.; Liu, L.; Chang, A.-m. (2007). Microwave hydrothermal synthesis of yttria stabilized zirconia at low temperature. *Weinadianzi Jishu*, 44(7/8), 76-79.

- Zheng, Y.; Tan, G.; Bo, H.; Miao, H.; Chang, M.; Xia, A. (2011). Effect of Tween 80 on preparation of BiFeO₃ in microwave-hydrothermal method. *Guisuanyan Xuebao*, 39(8), 1249-1253.
- Zheng, Ya-lin; Xu, G.-l.; Lai, Z.-yu; Liu, M. (2007). Effects of Cu content on the sintered properties of Ni-Cu-Zn ferrites. *Yadian Yu Shengguang*, 29(6), 707-709.
- Zhou, Y.; Yu, J.; Guo, M.; Zhang, M. (2010). Microwave hydrothermal synthesis and piezoelectric properties investigation of K_{0.5}Na_{0.5}NbO₃ lead-free ceramics. *Ferroelectrics*, 404, 69-75.
- Zhu, Z. F.; He, Z. L.; Li, J. Q.; Liu, D. G.; Wei, N. (2010). Synthesis and characterisation of fluorinated TiO₂ microspheres with novel structure by sonochemical-microwave hydrothermal treatment. *Materials Research Innovations*, 14(5), 426-430.